



Cite this: *Chem. Soc. Rev.*, 2023, 52, 4099

## Metallaphotoredox catalysis for $sp^3$ C–H functionalizations through hydrogen atom transfer (HAT)

Jingchang Zhang \*<sup>a</sup> and Magnus Rueping\*<sup>b</sup>

In recent years, the integration of photocatalytic hydrogen atom transfer (HAT) with transition metal catalysis has emerged as a formidable strategy for the construction of C( $sp^3$ )-carbon and C( $sp^3$ )-hetero bonds. The fusion of these two methodologies has been utilized widely in organic synthesis, leading to new transformations in chemical synthesis. In this review, we aim to summarize the recent advances made in  $sp^3$  C–H functionalizations through photocatalytic HAT followed by transition metal catalysis. Our focus will be on the diverse strategies and their synthetic applications, in addition to detailed mechanisms involved in these reactions. An in-depth understanding of these mechanisms is crucial for the rational design of new catalysts and reaction conditions to further enhance the efficiency of these transformations. We hope that this review will serve as a valuable resource for researchers in the area of metallaphotoredox catalysis, and will inspire the further development of this application in green chemistry, drug synthesis, material science, and other related fields.

Received 5th March 2023

DOI: 10.1039/d3cs00023k

[rsc.li/chem-soc-rev](https://rsc.li/chem-soc-rev)

<sup>a</sup> Department of Chemistry, School of Pharmacy, Jining Medical University, Rizhao 276826, China. E-mail: [zhangjingchang84@mail.jnmc.edu.cn](mailto:zhangjingchang84@mail.jnmc.edu.cn)

<sup>b</sup> KAUST Catalysis Center, KCC, King Abdullah University of Science and Technology, KAUST, Thuwal 23955-6900, Saudi Arabia. E-mail: [magnus.rueping@kaust.edu.sa](mailto:magnus.rueping@kaust.edu.sa)

### 1. Introduction

The formation of new C–carbon or C–hetero bonds from C–H bonds is a highly attractive synthetic strategy owing to the prevalence of C–H bonds in organic molecules. Consequently, transition metal-mediated C–H functionalizations have been



**Jingchang Zhang**

Jingchang Zhang received his BSc from Jinan University and his MSc from University of Science and Technology Liaoning. He obtained his PhD from Jilin University under the guidance of Professor Suoqin Zhang. In 2016, he began his independent research at Jining Medical University. His current research focuses on metallaphotoredox catalysis mediated  $sp^3$  C–H functionalization and bioactive molecules synthesis. Now, he is an associate professor at Jining Medical University.



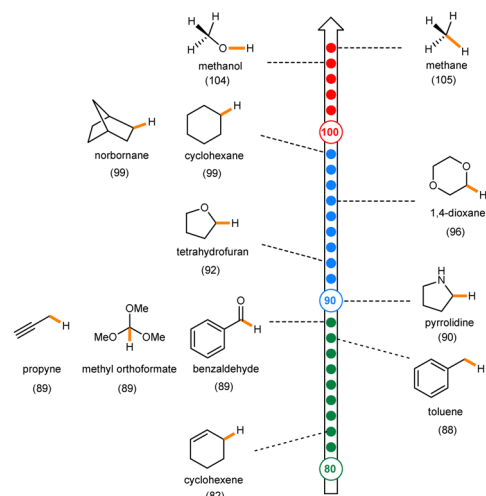
**Magnus Rueping**

Magnus Rueping obtained his doctoral degree from the ETH Zurich in 2002 working with Professor Dieter Seebach. He then moved to Harvard University to work with Professor David A. Evans. In 2004 he was directly appointed as Associate Professor at the University Frankfurt. After four years in Frankfurt, he accepted a Chair and Full Professorship of Organic Chemistry at RWTH Aachen University. He is currently Professor of Chemical and Biological Sciences at KAUST and the Associate Director of the KAUST Catalysis Center. His group's research activities are directed toward the development and simplification of catalytic methodology and technology, and their applications in the rapid synthesis of diverse functional natural and unnatural molecules.

the focus of organic chemists for several decades,<sup>1–8</sup> resulting in the development of a wide range of mature methodologies. These methods have been successfully employed in the construction of natural products and pharmaceuticals.<sup>9–11</sup> Despite the remarkable advances made in conventional transition metal-catalysed C–H functionalizations, the functionalization of sp<sup>3</sup> C–H bonds is still challenging. As a result, harsh conditions and directing groups are often required, leading to side-product generations and limited substrate scopes.<sup>12–14</sup> Overcoming these limitations and developing strategies for the conversion of sp<sup>3</sup> C–H bonds to other functional groups under mild conditions, with broad substrate scopes and a controllable selectivity, remains a significant challenge.

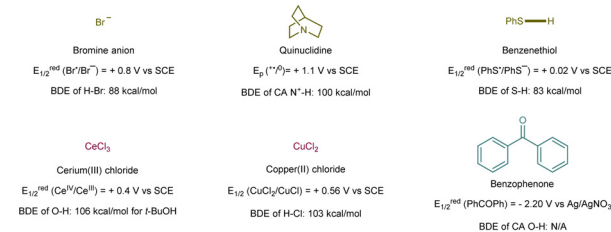
Recent developments in photochemistry have led to the emergence of photocatalysts (PC), such as acridiniums and iridium polypyridyl complexes (Scheme 1), which can generate open shell reactive species *via* single electron transfer (SET). These reactive species can be used to functionalize organic and organometallic substrates in solution, a task that would otherwise be difficult or impossible with other types of catalysts. Such strategies offer new possibilities for sp<sup>3</sup> C–H functionalizations with broader substrate scopes, mild reaction conditions, and a greater selectivity.<sup>15,16</sup>

Photocatalytic hydrogen atom transfer (HAT) is a noteworthy strategy for the activation of sp<sup>3</sup> C–H bonds, because it allows for the generation of a sp<sup>3</sup>-hybridized carbon-centered radical with a controllable selectivity as a C–H bond with the lowest bond dissociation energy (BDE) is activated (Scheme 2). There are several routes for the activation of a sp<sup>3</sup> C–H bond to result in an alkyl radical: the excited photocatalysts can facilitate SET to generate a hetero or halogen radical followed by HAT (indirect HAT); the excited transition metal photocatalysts can directly release a hetero or halogen radical *via* ligand-to-metal charge transfer (LMCT)-homolysis followed by HAT (LMCT HAT); and the excited photocatalysts can directly mediate HAT (direct HAT) (Scheme 3).<sup>17–20</sup> Importantly, these HAT processes can occur under very mild reaction conditions, such as at room temperature, which is particularly noteworthy.

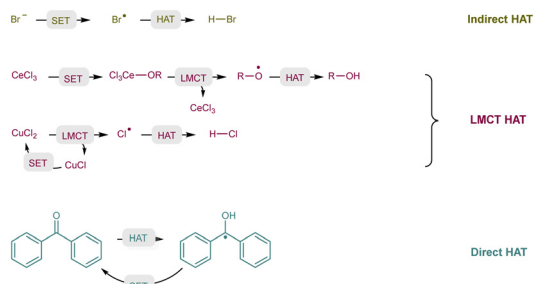


Scheme 2 Bond dissociation energies (kcal mol<sup>-1</sup>) of X–H bonds in representative compounds.

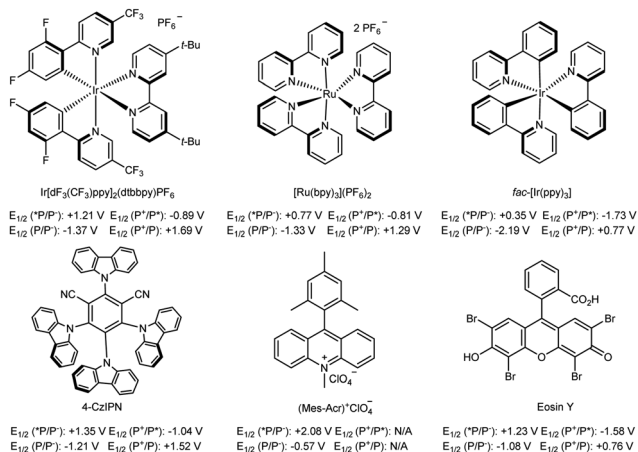
#### a. Representative HAT catalysts and BDEs of conjugate acids (CA)



#### b. Main HAT routes

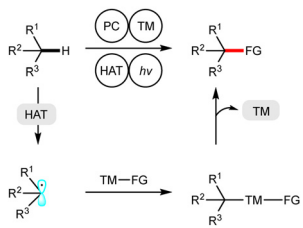


Scheme 3 Representative HAT catalysts and main HAT routes.

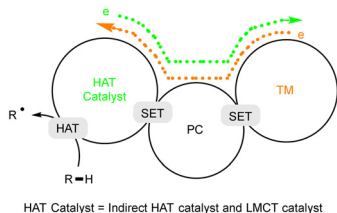


Scheme 1 Representative metallic and organic photocatalysts.

Over the past decade, metallaphotoredox catalysis has gained significant popularity in synthetic methodology.<sup>21–27</sup> This approach combines photocatalysis and transition metal catalysis to achieve the modular formation of C–carbon and C–hetero bonds. Specifically, the combination of photocatalytic HAT and transition metal catalysis has enabled the cross-coupling of sp<sup>3</sup> C–H bonds and other substrates through the generation of sp<sup>3</sup>-hybridized carbon centered radicals (Scheme 4a). This strategy opens up new possibilities for molecular constructions that were previously not feasible using either a photocatalyst or a transition metal catalyst alone. The success of this strategy relies on joint SET (electron transfer) between the HAT catalyst, photocatalyst and transition metal catalyst, which ensures the smooth progression of the reaction. The excited photocatalyst

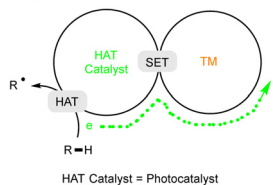
a.  $sp^3$  C-H functionalizations under metallaphotoredox catalysis through HAT

## b. Catalytic cycle for indirect HAT and LMCT HAT



HAT Catalyst = Indirect HAT catalyst and LMCT catalyst

## c. Catalytic cycle for direct HAT



HAT Catalyst = Photocatalyst

**Scheme 4**  $sp^3$  C-H functionalizations under the combination of photocatalytic HAT and transition metal catalysis as well as related catalytic cycles.

can act as an oxidant initially, and later delivers an electron to the transition metal catalyst after it is reduced (green line of Scheme 4b). Alternatively, if the excited state of the photocatalyst initially acts as a reductant, it takes an electron from the transition metal catalyst after it is oxidized (orange line of Scheme 4b). In cases where the photocatalyst is directly used as the HAT catalyst, it delivers an electron to the transition metal catalyst and releases a hydrogen proton to the reaction system after HAT. The sum of these two events, which do not occur simultaneously, is equivalent to the direct release of a hydrogen atom (Scheme 4c).

These different concepts of the combined use of photocatalytic HAT and transition metal catalysis clearly demonstrate the many possibilities of the application in synthesis and provide new opportunities for the development of  $sp^3$  C-H functionalizations. Therefore, it is not surprising that this area has emerged as an attractive and topical research field with growing applications in the synthesis of natural products and drugs. While some previous reviews have covered aspects of this field,<sup>28–31</sup> a comprehensive, detailed and systematic review is currently lacking.

This review aims to address this gap by providing a comprehensive overview of all direct  $sp^3$  C-H functionalizations mediated by the combination of photocatalytic HAT and transition metal catalysis. To achieve this, we classify the HAT catalysts and transition metal catalysis approaches used and highlight the cooperative principles of these catalysts. Moreover, we compare

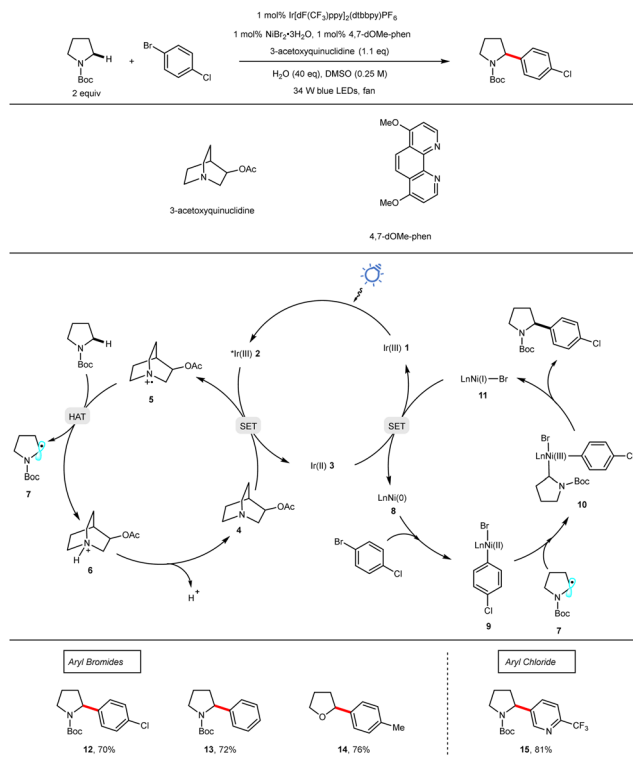
and contrast different transition metal catalysis approaches to provide readers with a deeper understanding of the similarities and differences between them. Our goal is to provide readers with an up-to-date and comprehensive understanding of the significance and potential of this research field. We hope this review will not only serve as a valuable resource for researchers and students working in this area but also facilitate the further development of this exciting and rapidly evolving field.

## 2. Hetero atom, halogen and carbon centered radicals as HAT catalysts

### 2.1 Hetero atom centered radicals as HAT catalysts

**2.1.1 Nickel catalysis.** Substantial efforts in the area of nickel catalysis have focused on coupling  $sp^3$ -hybridized fragments. Compared to palladium, nickel undergoes more rapid oxidative addition into alkyl halide bonds and suffers less from deleterious  $\beta$ -hydride elimination.<sup>32,33</sup> Photocatalysts, such as polypyridyl complexes of iridium or ruthenium, can be excited by low-energy visible light, with subsequent metal to ligand charge transfer (MLCT) followed by intersystem crossing (ISC), to provide a long-lived triplet excited state. This state has both a metal-centered vacancy that can oxidize a suitable electron donor and a  $\pi^*$ -centered unpaired electron that can reduce an adequate acceptor *via* SET.<sup>15</sup>

In 2016, MacMillan and co-workers demonstrated the arylation of the  $\alpha$  C-H bond of amides and ethers, as well as benzylic C-H bonds, by using an iridium polypyridyl complex, nickel, and 3-acetoxyquinuclidine (Scheme 5).<sup>34</sup> In this coupling, an amine radical cation (**5**) generated from the excited photocatalyst enabled SET oxidation of 3-acetoxyquinuclidine, will undergo a polarity-matched HAT to the  $\alpha$  C-H bond of amides and ethers to generate an alkyl radical. At the same time, the oxidative addition of a Ni(0) species (**8**) into an aryl halide electrophile affords a Ni(II) intermediate (**9**). The Ni(0) species (**8**) is generated *via* the independent two SET reductions of the initially employed Ni(II) catalyst by the reduced Ir-photocatalyst. Finally, alkyl radical capture by the Ni(II) intermediate (**9**) furnishes an Ni(III) intermediate (**10**). Subsequent reductive elimination affords the arylation product and Ni(I) species (**11**), which can be reduced by the Ir(III) complex (**3**) to regenerate both the Ni(0) species and Ir(III) photocatalyst. However, a DFT investigation suggests a reverse role of the Ni(I) species (**11**) that is similarly generated *via* the SET reduction of the initially employed Ni(II). Ni(I) (**11**) will firstly capture an alkyl radical to provide an alkyl Ni(II) bromide intermediate that upon a SET reduction by the reduced photocatalyst forms the Ni(I)-alkyl species, which subsequently undergoes oxidative addition with aryl bromides.<sup>35</sup> Excess 3-acetoxyquinuclidine is used as the HAT catalyst and base concurrently. A steric hindrance has a remarkable effect on this coupling. Aryl bromides and electron-deficient aryl chlorides are both good coupling partners with aryl bromides having a higher reactivity than aryl chlorides. If chlorine and bromine atoms are present, the chlorine atom will last after the coupling.

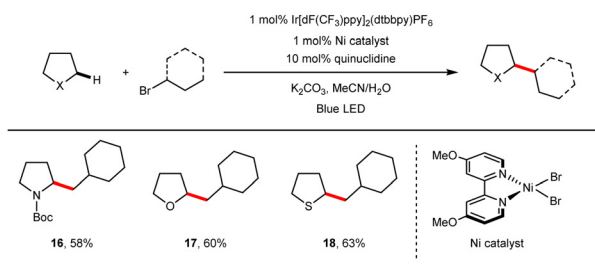
Scheme 5 Quinuclidine as HAT catalyst for  $sp^3$  C–H arylation.

This quinuclidine mediated HAT strategy was further applied into the  $\alpha$ -alkylation of amides, ethers and thioethers using alkyl bromides as coupling partners (Scheme 6a).<sup>36</sup> Besides, this strategy has been used in the direct arylation, vinylation and alkylation of aldehydes as well as the regioselective  $\alpha$ -arylation of alcohols in the presence of otherwise more hydridic C–H bonds (Scheme 6b and c).<sup>37,38</sup>

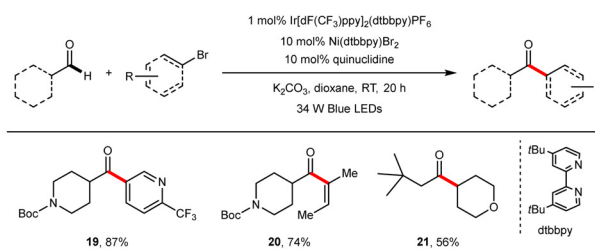
The use of HAT chemistry in the regioselective functionalization of remote  $C(sp^3)$ –H bonds in amines, amides, oximes, and alcohols has been an active area of research.<sup>39</sup> Rovis and colleagues have reported the alkylative cross-coupling between trifluoroacetamides and alkyl bromides using  $Ni(cod)_2$  or  $Ni(glyme)Cl_2$  as pre-catalysts, where a N-centered radical is generated *via* proton-coupled electron transfer (PCET), followed by 1,5-HAT to produce a carbon-centered radical.<sup>40</sup> Trifluoroacetamide serves as both the HAT catalyst and coupling substrate (Scheme 7a). The authors propose that the  $Ni(I)$  complex (**11**) plays a crucial role in the catalytic cycle, where the dihalogen  $Ni(III)$  intermediate (**27**) undergoes a SET reduction followed by the radical addition to give  $Ni(III)$  species (**29**) and reductive elimination to provide the product and  $Ni(I)$  catalyst.

In a similar work, Roizen and colleagues have reported the  $\gamma$ -arylation of sulfamate esters using 4-CzIPN as the photocatalyst in the combination with nickel through a 1,6-HAT process (Scheme 7b).<sup>41</sup> Meanwhile, Duan and colleagues have realized the  $\alpha$ -alkylation of amides and ethers using sulfonamide as a precursor for the formation of the corresponding N-centered radical *via* PCET, which can then perform HAT in an intermolecular fashion expanding the potential applicability (Scheme 7c).<sup>42</sup>

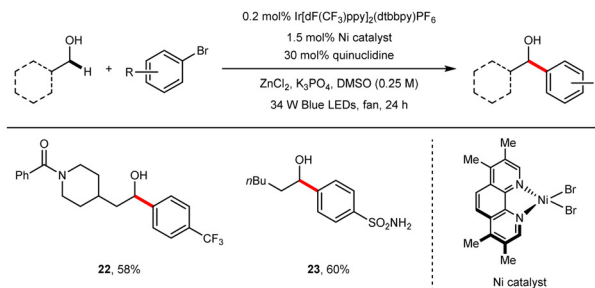
### a. Alkylation of polar $sp^3$ C–H



### b. Aldehyde C–H functionalization

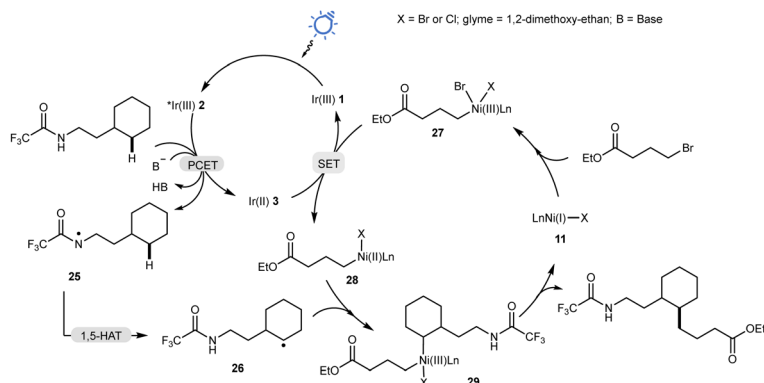
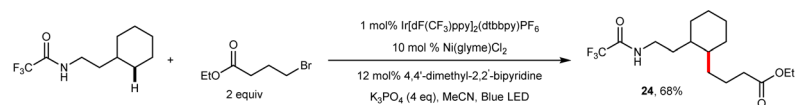
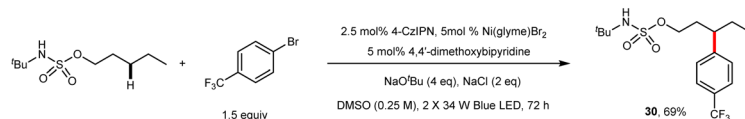
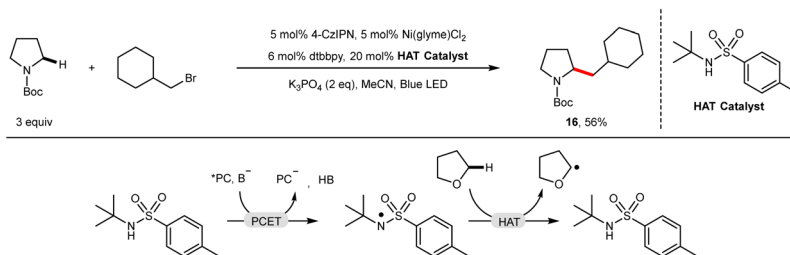


### c. $\alpha$ -Arylation of Alcohols



Scheme 6 Applications of Ir/Ni/quinuclidine strategy.

**2.1.2 Copper catalysis.** The combination of copper catalysis and photocatalysis has opened up new pathways for the formation of C–carbon and C–hetero bonds due to the favorable interaction of copper catalysts with radicals.<sup>43–45</sup> Zhu and colleagues disclosed the remote  $C(sp^3)$ –H functionalization of *N*-alkoxyppyridinium salts to obtain  $\delta$ -functionalized alcohols under Ir/Cu metallaphotoredox catalysis (Scheme 8a).<sup>46,47</sup> Various functionalizations, including azidation, cyanation, thiocyanation, arylation, and vinylation, have been achieved under similar conditions. In this transformation, an alkoxy radical, generated through the SET reduction of *N*-alkoxyppyridinium by  $Ir(ppy)_3$ , undergoes 1,5-HAT to yield a  $\delta$  carbon-centered radical, which is captured by ligand-exchanged  $Cu(II)$  salts ( $Cu(II)X$  or  $RCu(II)$ , **31** or **32**) to form  $Cu(III)$  intermediates (**33** or **34**). Subsequent reductive elimination leads to the formation of  $\delta$ -functionalized alcohols. *N*-Alkoxyppyridinium salts in this coupling serve as the substrate, HAT reagent, and oxidant simultaneously. Yu and colleagues later reported an asymmetric remote  $C(sp^3)$ –H bond cyanation of hydroxamides under similar conditions, with the inclusion of catalytic amounts of copper and a chiral ligand (Scheme 8b).<sup>48</sup>

a.  $\delta$ -Alkylation of amides through 1,5-HATb.  $\gamma$ -Arylation of sulfamate esters through 1,6-HATc. Sulfonamide as HAT catalyst for  $sp^3$  C-H alkylation

Scheme 7 Amides in HAT processes.

Nagib and colleagues reported the defluorination and remote dehydrogenation of *N*-fluoro-sulfonamides with the combination of Ir and copper catalysts, leading to the formation of  $\delta,\epsilon$ -unsaturated sulfonamides (Scheme 8c).<sup>49</sup> In this transformation, the SET reduction of *N*-fluoro-sulfonamide by the reduced photocatalyst generates a N-centered radical (42), followed by 1,5-HAT to generate a carbon-centered radical (43). This radical is then captured by Cu(II) to form a Cu(III) intermediate (44), which undergoes  $\beta$ -hydrogen elimination to afford  $\delta,\epsilon$ -unsaturated amines. This method is of relevance for the synthesis of both internal and terminal  $\delta$ -vinyl amines and aza-heterocycles.

**2.1.3 Cobalt catalysis.** Acridiniums exhibit strong oxidation properties in the singlet excited state (above 2.0 V for the singlet state), while their corresponding acridinyl radicals, formed through a SET reduction, act as moderate reductants (approximately  $-0.5$  V vs. SCE).<sup>16</sup> Anions such as  $\text{NO}_3^-$  ( $E^{\text{ox}}(\text{NO}_3^*/\text{NO}_3^-) = +1.97$  V vs. SCE) and  $\text{Cl}^-$  ( $E^{\text{ox}}(\text{Cl}^*/\text{Cl}^-) = +2.03$  V vs. SCE) can be oxidized by acridiniums to generate their respective radicals, enabling HAT to alkanes.<sup>50,51</sup>

Cobaloximes, which contain a Co(II) center, are capable of trapping alkyl radicals to form Co(III)-alkyl complexes. Upon photolysis, these complexes can undergo  $\beta$ -hydrogen elimination to produce Co(III)-H and olefins as the elimination products.<sup>52-57</sup>

Through the combination of acridinium and cobaloxime catalysis, Nicewicz and colleagues developed a homobenzylic oxygenation reaction (Scheme 9).<sup>50</sup> The cobaloxime catalyst facilitates the hydrogen evolution and turnover of the photocatalyst by oxidizing the acridinyl radical. Styrene derivatives, formed from the starting alkanes, serve as intermediates in this reaction and are further converted into propiophenone products.  $\text{LiNO}_3$  is used as a HAT reagent for substrates that are unfavorable for a SET oxidation, triggering initial benzylic C-H HAT. However, electron-rich substrates that can undergo a direct SET oxidation by acridiniums can also be efficiently converted in the absence of  $\text{LiNO}_3$ , showcasing broader functional group tolerances.

**2.1.4 Chromium catalysis.** The chromium-mediated allylation of aldehydes is a valuable method to selectively allylate



with the chromium(III) complex, thereby restoring both acridinium and chromium(II) catalysts. The introduction of a chiral ligand enables the synthesis of enantiomerically and diastereomerically enriched homoallylic alcohols. The same group has further disclosed the alkylation of ketones to afford tertiary alcohols under very similar conditions, wherein a titanium(III) catalyst is used instead of the chromium(II) catalyst and SET between a Ti(IV) species and acridinyl radical will regenerate both initial catalysts ( $E_{\text{red}}(\text{CpTiCl}_3) = -0.35 \text{ V vs. SCE}$ ) (Scheme 10b).<sup>65</sup>

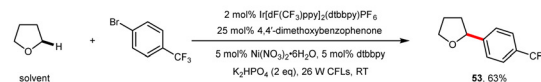
## 2.2 Halogen atom radicals in HAT processes

The bromine anion exhibits a moderate redox potential ( $E_{1/2}^{\text{red}}(\text{Br}^\bullet/\text{Br}^-) = +0.8 \text{ V vs. SCE}$  in DME),<sup>66</sup> and plays a crucial role in the HAT-based coupling reactions of aryl and alkyl bromides under metallaphotoredox catalysis. There are two potential pathways for the generation of a bromine radical: the direct SET oxidation of a bromine anion by an excited photocatalyst and the homolysis of a Ni(II)-Br bond in a triplet state (see Section 3). Once formed, the bromine radical selectively engages in HAT with polar  $\text{sp}^3 \text{ C-H}$  bonds.

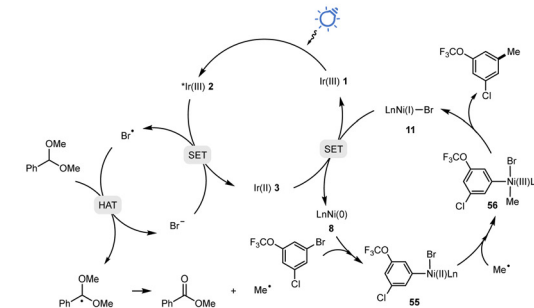
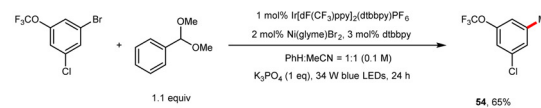
**2.2.1 Nickel catalysis.** In 2016, Molander and colleagues reported the cross coupling between ethers and aryl bromides (Scheme 11a).<sup>67</sup> While various mechanistic pathways have been proposed, the observed kinetic isotope effect (KIE) and limited reactivity of stronger C-H bonds strongly suggest the involvement of bromine radicals in the HAT process. For instance, Doyle and co-workers described the methylation of aryl bromides mediated by metallaphotoredox catalysis using benzaldehyde dimethyl acetal as the methyl source (Scheme 11b).<sup>68</sup> The oxidative addition of the Ni(0) species (**8**) into aryl bromides leads to the formation of Ni(II) intermediates (**55**). A bromine radical, generated through the direct SET oxidation of a bromine anion by the excited Ir(III) photocatalyst, selectively performs HAT to the tertiary C-H bond of benzaldehyde dimethyl acetal. The subsequent  $\beta$ -scission leads to the methyl radical and methyl benzoate. The methyl radical is trapped by Ni(II) intermediates (**55**), forming Ni(III) intermediates (**56**) that readily undergo reductive elimination, resulting in the formation of C(sp<sup>2</sup>)-C(sp<sup>3</sup>) bonds and the Ni(I) complex (**11**). Reduced Ir(II) photocatalyst then reduces the Ni(I) species, regenerating both the Ir(III) and Ni(0) catalyst. The generation of methyl benzoate, radical clock experiments, methyl radical trapping experiments, and the essential role of bromine radical-mediated HAT and the methyl radical generation in this reaction. Sulfonyl aziridines also serve as suitable coupling partners under similar conditions, leading to the synthesis of valuable  $\beta$ -methylated (alkylated) sulfonamides upon ring opening (Scheme 11c).<sup>69</sup>

Martin and colleagues have introduced a protocol for the  $\alpha$  C(sp<sup>3</sup>)-H arylation and alkylation of benzamides (Scheme 11d).<sup>70</sup> This method utilizes a wide range of aryl- and heteroaryl-substituted bromides, as well as various alkyl bromides, to afford  $\alpha$ -arylated and alkylated benzamides in moderate to good yields. Enantioselective C-H functionalizations have also been achieved through the incorporation of a chiral ligand. Related mechanistic studies conducted by Montgomery and

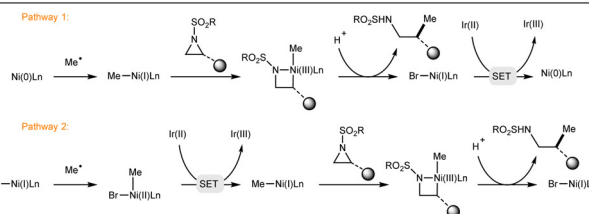
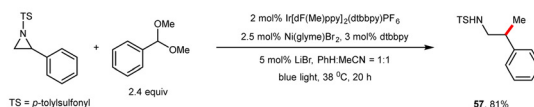
### a. Coupling between aryl bromides and $\text{sp}^3 \text{ C-H}$



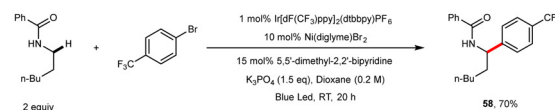
### b. Methylation of aryl bromides



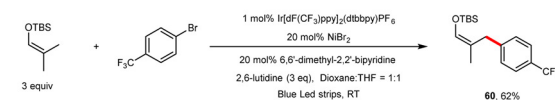
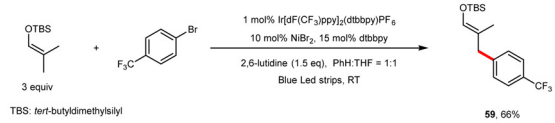
### c. Methylation of sulfonyl aziridines



### d. $\alpha$ C-H arylation and alkylation of benzamides



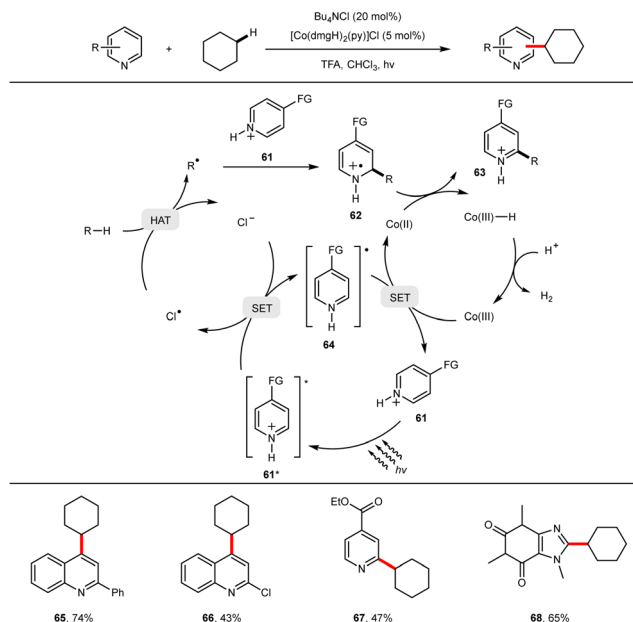
### e. Stereoselectivity regulatable allylic $\text{sp}^3 \text{ C-H}$ arylation



Scheme 11 Bromine radical in HAT processes.

co-workers support the involvement of bromine radical-mediated HAT as the plausible mechanism (Scheme 11d).<sup>71</sup>

In a recent development, Rueping and co-workers reported an allylic C(sp<sup>3</sup>)-H arylation protocol with tunable stereoselectivities under Ir/Ni dual catalysis (Scheme 11e).<sup>72</sup> This innovative approach enables the direct catalytic generation of allylic radicals from readily available alkenes and allows for the coupling with a broad range of aryl halides. Computational studies have revealed that the excitation of a Ni(II)-allyl complex from a singlet



Scheme 12 Cobaloxime mediated cross dehydrogenative coupling.

state to a triplet state triggers a spontaneous change in the allyl group coordination. By employing different ligands, isomerization can be selectively directed, thereby achieving a controllable *E/Z* selectivity. The ability to modulate an allylation stereoselectivity through ligand switches presents a promising strategy for accessing both *E* and *Z* isomers in target synthesis.

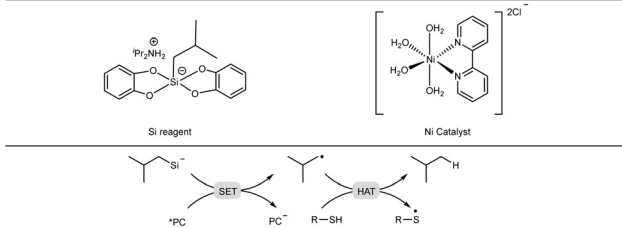
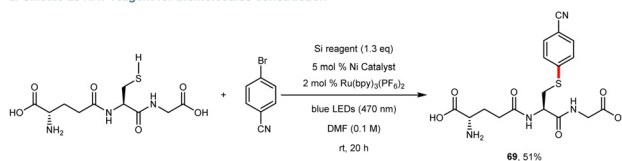
**2.2.2 Cobalt catalysis.** Li and colleagues have reported an intriguing cobaloxime-mediated cross dehydrogenative coupling (CDC) strategy that enables the coupling of alkanes and heteroarenes (Scheme 12).<sup>73</sup> In this transformation, a trifluoroacetic acid protonated heteroarene (**61**) serves as a photooxidant, facilitating the generation of a chlorine radical for HAT to generate an alkyl radical which adds to another protonated heteroarene (**61**), leading to the formation of a radical cation intermediate (**62**). Subsequently, the Co(II) catalyst facilitates the hydrogen atom removal from this intermediate, resulting in the desired alkylated heteroarene (**63**) and a Co(III)-H species. Co(III)-H is then protonated to generate Co(III) under the H<sub>2</sub> evolution. Importantly, the regeneration of both the Co(II) catalyst and protonated heteroarene (**61**) occurs through SET between the heteroarene radical intermediate (**64**) and Co(III). The presence of alkyl and chlorine radicals is supported by radical capture experiments, providing valuable insights into the reaction mechanism. Further investigations have convincingly ruled out the possibility of the chlorine radical generation from the cobaloxime catalyst. Moreover, the strong interaction between excited heteroarenes and chlorine anions is observed only in the presence of an acid, emphasizing the indispensable role of trifluoroacetic acid in protonating heteroarenes for the chlorine anion oxidation.

## 2.3 Carbon centered radicals for HAT

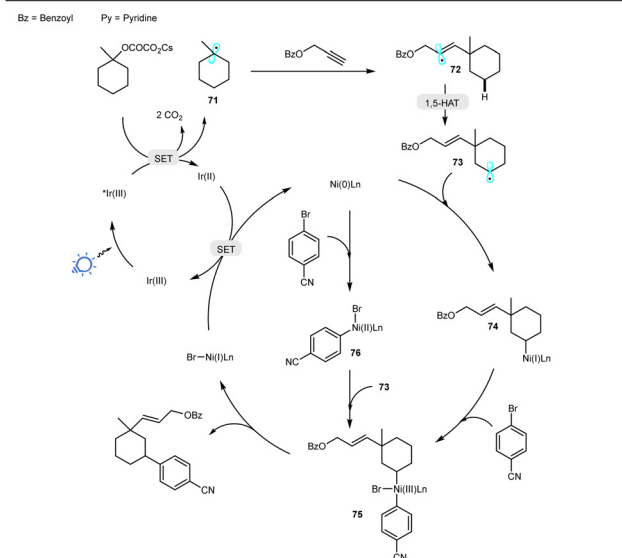
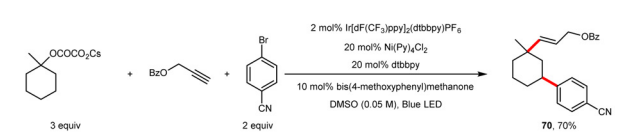
**2.3.1 Nickel catalysis.** Alkyl radicals are known to exhibit a reactivity towards weaker carbon-hydrogen or hetero-hydrogen

bonds through HAT processes. However, alkyl radicals can not be directly generated from C(sp<sup>3</sup>)-H bonds through SET oxidation or reduction pathways, and they are not recyclable after HAT. To generate alkyl radicals, alkylsilicates can undergo a SET oxidation by an excited photocatalyst due to their moderate redox potentials (average *E*<sub>0</sub> = +0.75 V vs. SCE for 1° alkylsilicates). Taking the advantage of this property, Molander and colleagues developed a selective thioetherification strategy for constructing peptides and other biomolecules by cross-coupling thiols and aryl bromides (Scheme 13a).<sup>74,75</sup> This methodology employs an excess (1.2–1.5 equiv.) of ammonium bis(catechol)isobutylsilicate as a HAT reagent. Notably, various functional groups such as unprotected carboxyl, amino, hydroxy, amide, and sulfonamide are tolerated under these coupling conditions.

### a. Silicate as HAT reagent for biomolecules construction



### b. Three component reaction through intramolecular 1,5-HAT



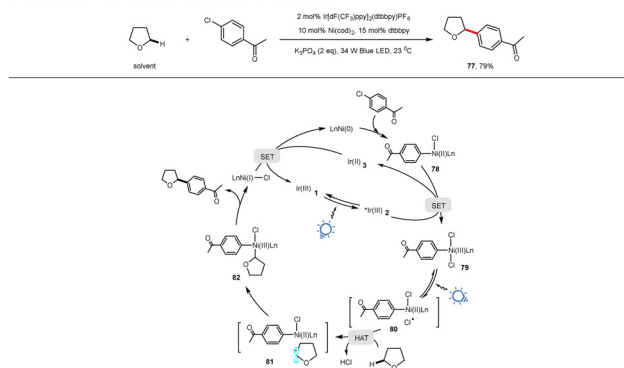
Scheme 13 Carbon-centered radicals in HAT processes.

In a related study, Chu and co-workers reported a three-component decarboxylative vinylation/remote C(sp<sup>3</sup>)-H bond arylation process for the synthesis of 1,3-disubstituted cycloalkanes (Scheme 13b).<sup>76</sup> The reaction involves the SET oxidation of oxalate, followed by decarboxylation, to generate a tertiary alkyl radical (71). This radical then adds to an alkyne to form a vinyl radical (72), which subsequently undergoes intramolecular 1,5-HAT to generate a secondary alkyl radical (73). The latter is captured by a Ni(0) species to form an alkyl Ni(I) intermediate (74). The oxidative addition by aryl bromides to the alkyl Ni(I) intermediate yields aryl alkyl Ni(III) complexes (75), which undergo reductive elimination to afford 1,3-disubstituted cycloalkanes. The authors propose an alternative mechanistic pathway involving the oxidative addition of Ni(0) into the aryl bromides to form Ni(II) intermediates (76), followed by the trapping of the alkyl radical (73) to generate aryl alkyl Ni(III) complexes (75). This versatile protocol offers the potential to construct bioactive molecules from simple substrates and exhibits a broad substrate scope encompassing various oxalates, alkynes, and (hetero)aryl halides.

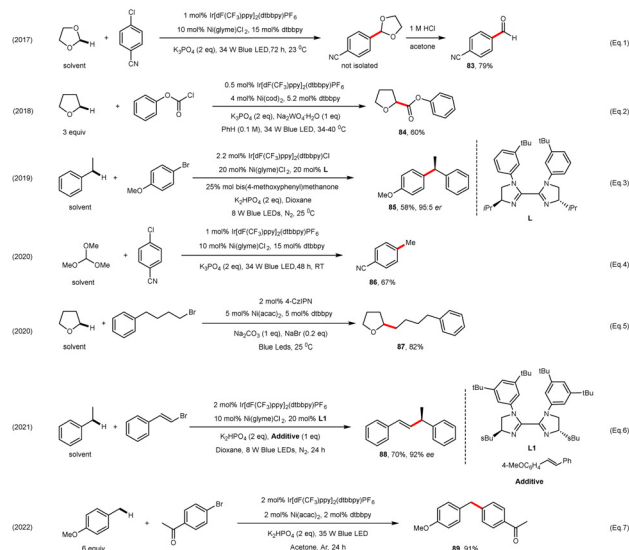
### 3. Halogen photoelimination processes

Photoinduced ligand to metal charge transfer (LMCT) processes have emerged as efficient strategies for alkane HAT, leading to the generation of alkyl radicals. In particular, photoexcitation-LMCT-homolysis (PE-LMCT-HM) has proven effective in the direct release of halogen and alkoxy radicals from metal salts, such as Cu(II), Fe(III), and Ce(IV). This process overcomes the challenges associated with photoredox-induced SET pathways (see Scheme 3).<sup>77–79</sup> Inspired by the pioneering work of Nocera and colleagues on the photoinduced liberation of halogen radicals from high-valent Ni(III) halide complexes,<sup>80,81</sup> Doyle and co-workers developed a halogen photoelimination strategy for the cross-coupling of ethers and aryl chlorides (Scheme 14a).<sup>82</sup> The key step in this coupling involves the generation of a high-valent Ni(III) intermediate, specifically the dichloride Ni(III) complex. The oxidative addition of Ni(0) to aryl chlorides readily yields aryl chloride Ni(II) intermediates (78), which are subsequently converted to dichloride Ni(III) complexes (79) through a SET oxidation enabled by an excited photocatalyst. Under visible light irradiation, the dichloride Ni(III) complex undergoes photoexcitation-LMCT-homolysis, resulting in the release of a chlorine radical. This chlorine radical effectively performs HAT on alkanes. The rapid rebound of the HAT-generated alkyl radical to the Ni center gives rise to alkyl aryl Ni(III) complexes (82), which undergo reductive elimination to afford  $\alpha$ -arylated ethers. The SET reduction of Ni(II) by Ir(II) facilitates the regeneration of the Ni(0) species and Ir(III) photocatalyst. Control experiments employing stoichiometric (dtbbpy)Ni<sup>III</sup>(Ar)(Cl) (Ar = 4-methylphenyl) and single-electron oxidant tris(4-bromophenyl)ammoniumyl hexachloroantimonate ([TBPAA]SbCl<sub>6</sub>) under visible light irradiation demonstrate that the absence of the oxidant or light results in no product

a. Halogen photoelimination strategy for coupling of aryl chlorides and sp<sup>3</sup> C-H



b. Applications of halogen photoelimination strategy



Scheme 14 Halogen photoelimination strategy and applications.

formation, indicating the generation of Ni(III) chloride complexes. Deuterium labeling experiments conducted with aryl halides and THF-d<sub>8</sub> provide the evidence against the Ni(III)-Ar bond homolysis of 79, thereby suggesting the presence of chlorine radicals. Additional mechanism studies carried out in this research further support the feasibility of chlorine photoelimination.<sup>83</sup> Given the good HAT efficiency of a halogen radical, this strategy has broad applications and can be applied to different functionalizations, including the arylation (Scheme 14b, Eq (1), (3), (4) and (7)), esterification (Scheme 14b, Eq (2)), chloroformates as coupling partner), alkylation (Scheme 14b, Eq (5)) and vinylation (Scheme 14b, Eq (6)), of various sp<sup>3</sup> C-H bonds.<sup>84–90</sup>

A noteworthy development by Wu and co-workers involved the hydroalkylation of alkynes utilizing ethers and amides as alkyl sources under photoredox/Ni catalysis (Scheme 15a).<sup>91</sup> The proposed mechanism suggests that the employed Ni(II) catalyst undergoes a SET oxidation by the excited photocatalyst, generating a Ni(III) species. Subsequently, the Ni(III) species releases a chlorine radical *via* PE-LMCT-HM, enabling HAT to alkanes (in line with the findings of Nocera and Doyle). This methodology exhibits a broad substrate scope, delivering hydroalkylation products with an excellent *E* selectivity.

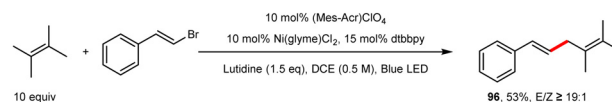
However, terminal alkynes are unsuitable substrates due to their propensity for the competitive [2+2] cycloaddition.

In a separate study, Hong and co-workers reported the C(sp<sup>3</sup>)-H acylation using *N*-acylsuccinimides (Scheme 15b).<sup>92</sup> Supported by DFT calculations and control experiments, the authors proposed a pivotal Ni(III) trichloride intermediate (92) that undergoes HAT to generate an alkyl Ni(III) intermediate (93). Sequential SET reductions lead to the formation of an alkyl Ni(I) species (94), facilitating the oxidative addition to *N*-acylsuccinimides. Notably, the utilization of acyl chlorides as coupling partners has been proved to be less effective, resulting in significantly lower yields compared to *N*-acylsuccinimides.

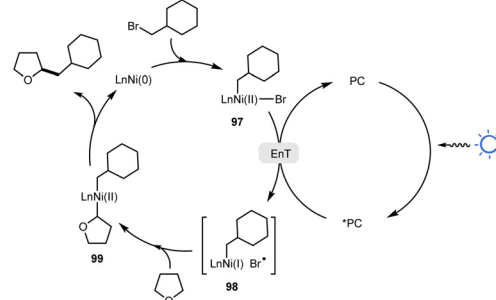
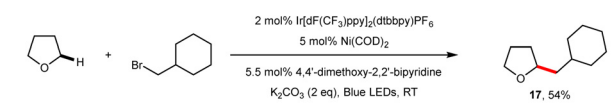
Rueping and co-workers have made significant contributions in the field of the direct regioselective coupling of allylic C(sp<sup>3</sup>)-H bonds with aryl and vinyl bromides by employing a combination of nickel and photoredox catalysis (Scheme 16a).<sup>93</sup> This new methodology enables the synthesis of allylarenes and 1,4-dienes from unactivated alkenes under mild reaction conditions. The authors proposed an energy transfer (EnT) pathway, where the homolysis of the Ni(II)-Br bond in an aryl Ni(II) bromide intermediate leads to the release of a bromine radical, facilitating HAT to allylic C-H bonds.

Furthermore, Rueping and co-workers extended their research on the cross-coupling of sp<sup>3</sup> C-H bonds and alkyl bromides by developing the EnT-enabled Ni(II)-Br homolytic process supported

a. Cross coupling between allylic sp<sup>3</sup> C-H and vinyl bromides



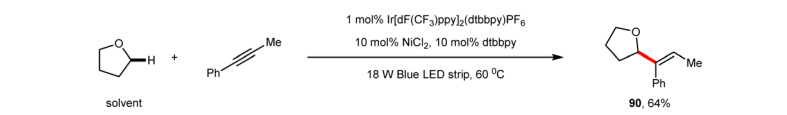
b. Cross coupling between sp<sup>3</sup> C-H and alkyl bromides



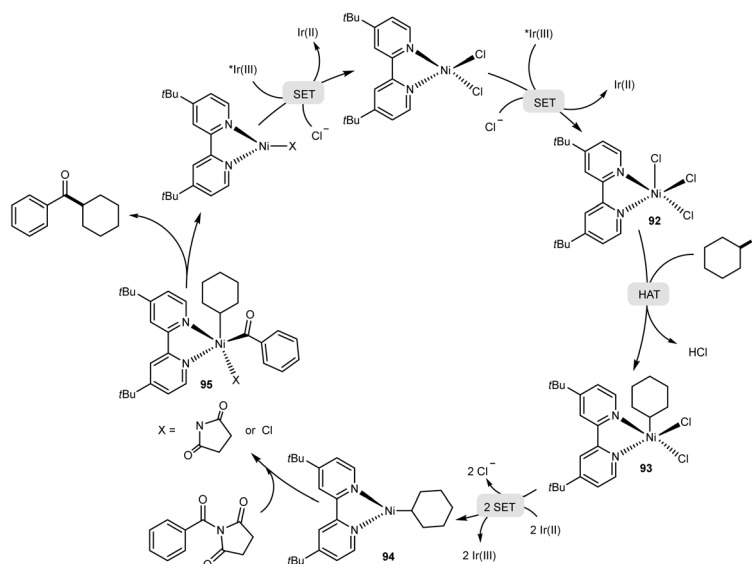
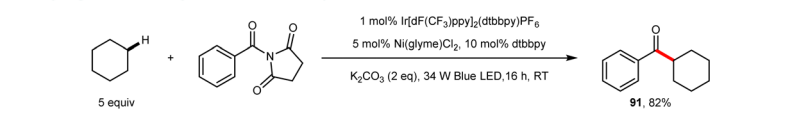
Scheme 16 Ni(II)-Br homolysis pathway through energy transfer.

by experimental, computational, and spectroscopic studies (Scheme 16b).<sup>94</sup> They suggested a Dexter triplet-triplet energy

a. Regioselective hydroalkylation of internal alkynes



b. Coupling between *N*-acylsuccinimides and sp<sup>3</sup> C-H

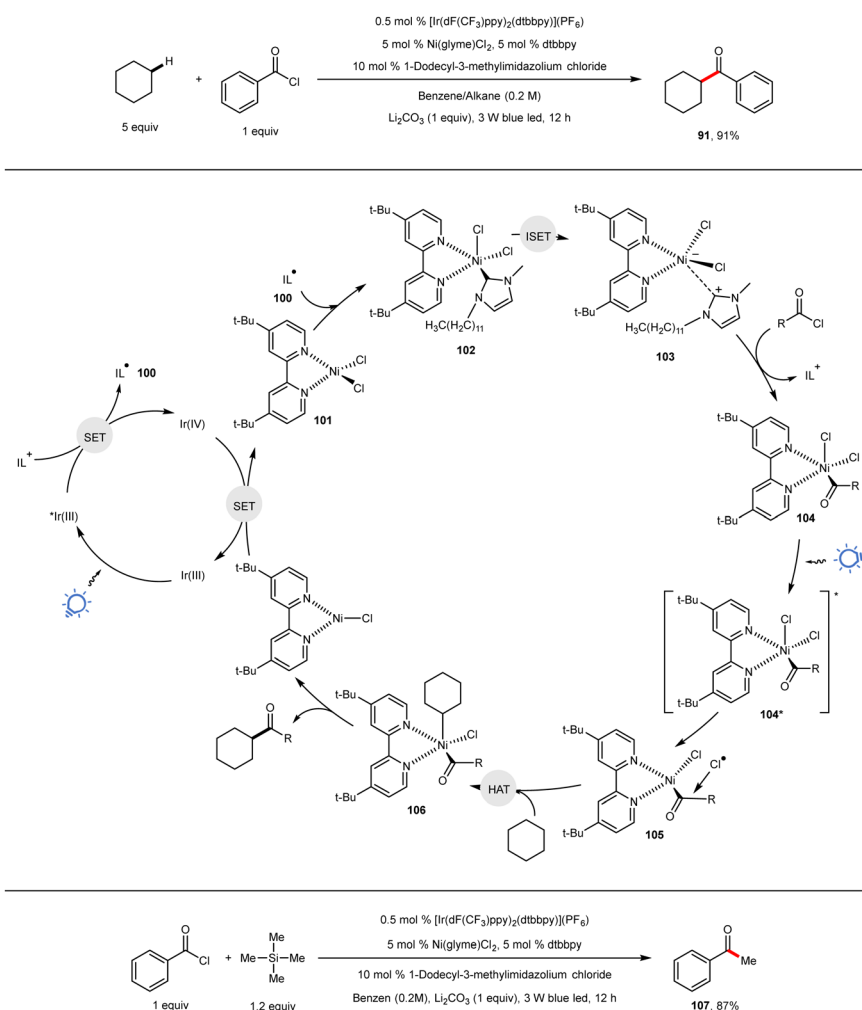


Scheme 15 Ni(III) trichloride mediated chlorine radical photoelimination.

transfer (EnT) from the excited photocatalyst to the alkyl Ni(II) bromide intermediate (**97**). This results in the formation of the Ni(II) triplet state, which subsequently undergoes the homolysis of the Ni(II)–Br bond, liberating a bromine radical. Subsequent HAT and reductive elimination yield the desired product and Ni(0) species. Mechanistic investigations revealed that the Ni(III)–Br homolysis pathway is unfavorable due to the high-energy barrier associated with the following C(sp<sup>3</sup>)–H activation ( $\Delta G^\ddagger = 45.9 \text{ kcal mol}^{-1}$ ). This study provides valuable insights into photoredox/Ni catalysis pathways. As such, for sp<sup>3</sup> C–H functionalizations involving aryl and alkyl bromides under photoredox/Ni catalysis, both the direct oxidation pathway of the bromine anion (see 2.2) and the Ni(II)–Br homolytic pathway are viable routes.

Zhang and co-workers have made significant strides in the field by developing an innovative triple catalysis strategy mediated by an ionic liquid. This strategy enables the direct formation of dihalogen Ni(III) complexes through the oxidative addition of a pseudo Ni(I) complex (Scheme 17).<sup>95</sup> Leveraging this approach, they have achieved high-yielding direct couplings between acyl chlorides and highly polar or strong C(sp<sup>3</sup>)–H

bonds, as well as the one-pot methylation of acyl chlorides using only 1.2 equivalents of tetramethylsilane as the methyl source, involving successive C(sp<sup>3</sup>)–H and C(sp<sup>3</sup>)–Si cleavage steps. In this strategy, the visible light irradiation of an Ir(III) complex generates an excited species, which is subsequently oxidized by an ionic liquid cation, leading to the formation of an ionic liquid radical (**100**) and an Ir(IV) complex. The ionic liquid radical then combines with Ni(II) (**101**) to generate a Ni(III) complex (**102**), followed by intramolecular single-electron transfer (ISET), resulting in the formation of a pseudo Ni(I) complex (**103**). This pseudo-Ni(I) complex exhibits an ionic-type bond, wherein the electropositive ionic liquid moiety binds to the electronegative Ni-complex moiety. The oxidative addition of the pseudo Ni(I) complex by acyl chlorides yields acyl dichloride Ni(III) complexes (**104**), with the concomitant release of the ionic liquid cation. The subsequent visible light irradiation of an acyl dichloride Ni(III) complex leads to the liberation of a chlorine radical through photoexcitation-ligand to metal charge transfer-homolysis (PE–LMCT–HM), that can undergo HAT to the alkane resulting in the formation of an acyl alkyl Ni(III) species (**106**). The reductive elimination of the acyl alkyl Ni(III) species affords the



Scheme 17 Ir/Ni/ionic liquid catalyzed alkylation and one pot methylation of acyl chlorides.

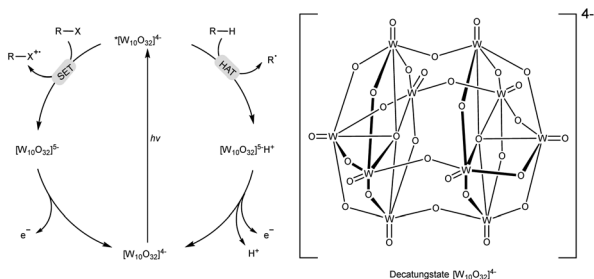
desired product and Ni(II) complex. The Ni(II) complex is then efficiently regenerated through the SET oxidation of the Ni(I) complex by the Ir(IV) complex. Notably, unlike other photoredox/Ni mechanisms where a Ni(0) or Ni(I) complex serves as the active species, in this research, the pseudo Ni(I) complex, generated from the initially employed Ni(II) catalyst with the assistance of an ionic liquid, plays a pivotal role.

## 4. Decatungstate as photocatalyst and HAT reagent

The photochemical behavior of decatungstate  $[W_{10}O_{32}]^{4-}$  (DT) upon the absorption of a UV photon has been extensively investigated, revealing an oxygen-to-metal charge-transfer (LMCT) character. Nano and microsecond laser flash photolysis (LFP) experiments have confirmed the rapid decay of the excited state, leading to the formation of a dark state **wO**. This **wO** species possesses an electron-deficient oxygen center, exhibiting an oxyradical-like character. It is considered the chemically active species with a predicted  $E(\mathbf{wO}/[W_{10}O_{32}]^{5-})$  value of approximately +2.44 V vs. SCE.<sup>96</sup> Thus, **wO** can engage in the SET oxidation of R-X substrates, particularly those that are easily oxidizable or lack a weak R-H bond, resulting in the formation of radical cations ( $R-X^{\bullet+}$ ). Additionally, **wO** can undergo HAT reactions with alkanes, generating alkyl radicals (Scheme 18). Consequently, decatungstate has found applications as an efficient HAT photocatalyst for the oxygenation, dehydrogenation, conjugate addition, and fluorination of strong  $C(sp^3)$ -H bonds.<sup>97</sup>

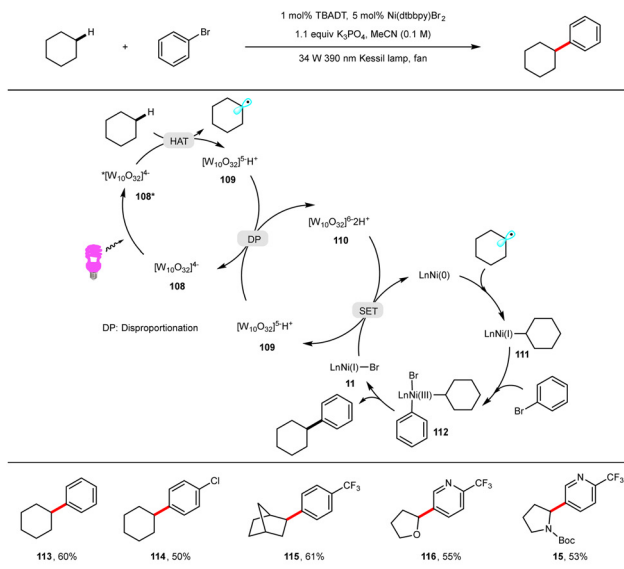
### 4.1 Nickel catalysis

In 2018, MacMillan and co-workers successfully employed decatungstate in the combination with nickel catalysis for the direct arylation of highly polar and strong  $sp^3$  C-H bonds (Scheme 19a).<sup>98</sup> In this transformation, excited decatungstate (**108\***) abstracts a hydrogen atom from an inert alkane, such as cyclohexane, yielding a singly reduced decatungstate complex (**109**) and a carbon-centered radical. The disproportionation (DP) of two singly reduced decatungstate complexes leads to the regeneration of decatungstate (**108**) and the formation of a doubly reduced decatungstate species (**110**). Simultaneously, the alkyl radical reacts with the Ni(0) species, forming a Ni(I)-alkyl species (**111**). The oxidative addition of the Ni(I)-alkyl species (**111**) with aryl bromides generates aryl alkyl Ni(III)

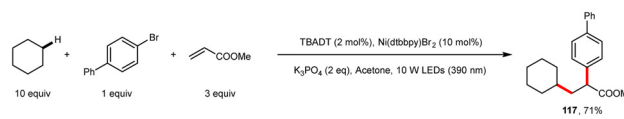


Scheme 18 Pathways of excited decatungstate to activate substrates.

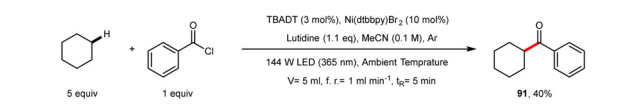
#### a. Arylation of very strong and polar $sp^3$ C-H



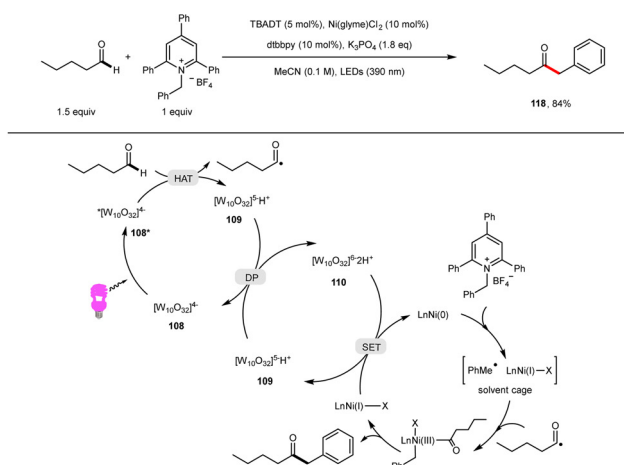
#### b. Difunctionalization of alkenes



#### c. Acylation of $sp^3$ C-H in a continuous flow



#### d. Cross coupling between aldehydes and alkyl pyridinium salts



Scheme 19 Decatungstate/Ni metallaphotoredox catalysis and applications.

species (**112**), which subsequently undergo reductive elimination to produce cross-coupling products and the Ni(I) species (**11**). It has been suggested that final SET between the Ni(I) species and the doubly reduced decatungstate species (**110**) regenerates the active Ni(0) species ( $E_p(\text{Ni}^{\text{II}}/\text{Ni}^{\text{0}}) = -1.47$  V vs.  $\text{Ag}/\text{Ag}^+$  in MeCN, ( $E_{1/2}^{\text{red}}([W_{10}O_{32}]^{5-}/[W_{10}O_{32}]^{6-}) = -1.52$  V vs.  $\text{Ag}/\text{Ag}^+$  in MeCN)).<sup>99</sup> Building upon this strategy, Kong and

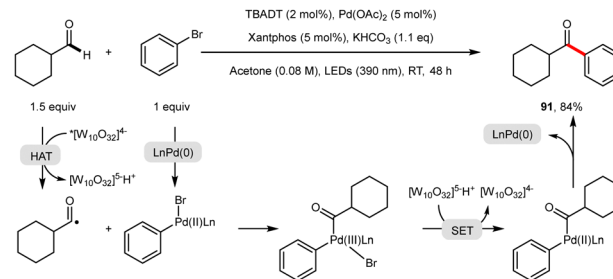
co-workers applied it to the three-component difunctionalization of alkenes, demonstrating its utility in the selective late-stage functionalization of complex natural products and the concise synthesis of pharmaceutically relevant molecules (Scheme 19b).<sup>100</sup> In addition, Noël and co-workers reported the C(sp<sup>3</sup>)-H acylation and arylation in a continuous flow, offering significantly reduced reaction times compared to traditional batch reactions (Scheme 19c).<sup>101</sup> Furthermore, Rasappan and co-workers reported the alkylation of aldehydes using alkyl pyridinium salts as coupling partners in the presence of decatungstate and nickel catalysis, wherein decatungstate-mediated HAT generates acyl radicals (Scheme 19d).<sup>102</sup>

## 4.2 Copper catalysis

Copper catalysts have demonstrated a remarkable efficacy in trifluoromethylation reactions.<sup>103,104</sup> MacMillan and co-workers successfully employed decatungstate in the combination with a copper catalyst to achieve the trifluoromethylation of sp<sup>3</sup> C-H bonds using Togni reagent as the trifluoromethyl source (Scheme 20).<sup>105</sup> The reduction of the trifluoromethylation reagent by the singly reduced decatungstate complex (**109**) in the presence of Cu(I) leads to the formation of a Cu(II)-CF<sub>3</sub> intermediate (**119**). The subsequent capture of an alkyl radical by the Cu(II)-CF<sub>3</sub> intermediate generates a key alkyl-Cu(III)-CF<sub>3</sub> complex (**120**), which undergoes reductive elimination to deliver the desired C(sp<sup>3</sup>)-CF<sub>3</sub> product, while regenerating the Cu(I) catalyst. This trifluoromethylation strategy exhibits a broad applicability and is compatible with various C(sp<sup>3</sup>)-H bonds. Importantly, free amino, amide, sulfamide, and carboxyl functionalities are all well-tolerated in this coupling.

## 4.3 Palladium catalysis

The coupling of aldehydes and aryl halides under palladium catalysis represents an efficient route to access ketones.<sup>106</sup>

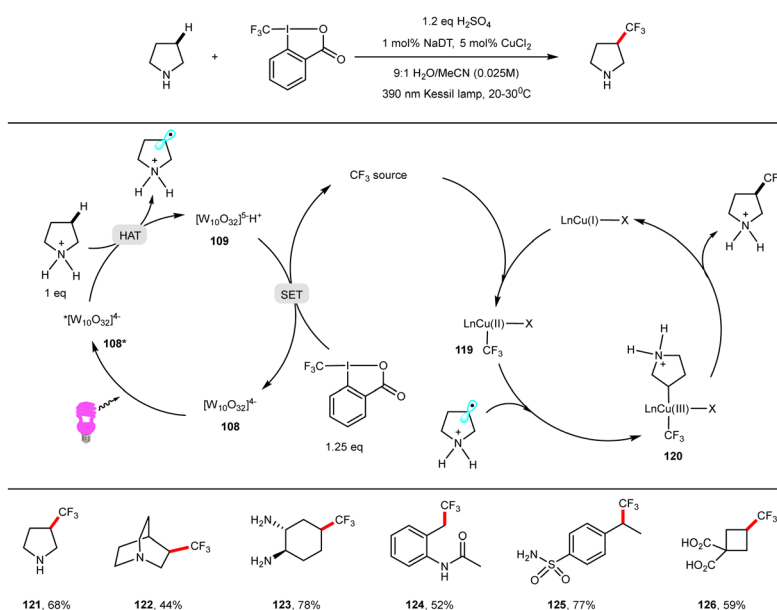


Scheme 21 Decatungstate/Pd catalysed synthesis of ketones.

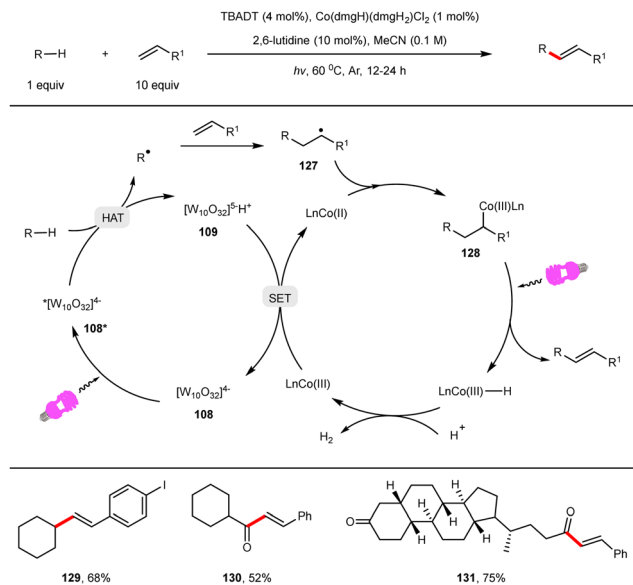
Zheng and co-workers reported the arylation of aldehyde C-H bonds using aryl bromides as coupling partners in the presence of decatungstate and a palladium catalyst (Scheme 21).<sup>107</sup> In this process, decatungstate facilitates hydrogen atom abstractions to form acyl radicals, while palladium activates aryl bromides, generating aryl Pd(II) bromide intermediates.

## 4.4 Cobalt catalysis

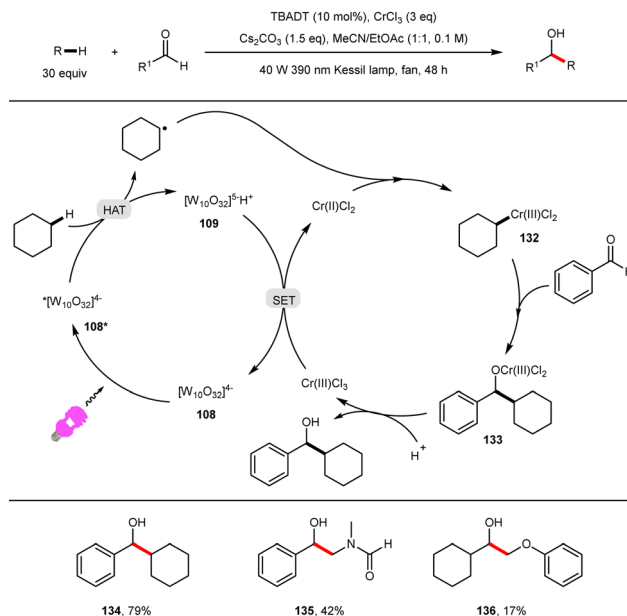
In a pioneering work Sorensen and co-workers demonstrated an important approach by combining decatungstate and a cobaloxime pyridine chloride complex for the dehydrogenation of alkanes to alkenes and the dehydrogenation of alcohols to ketones.<sup>108</sup> Building upon this work, Wu and co-workers reported the site-selective alkenylation of alkanes and aldehydes (Scheme 22).<sup>109</sup> Photoexcited decatungstate (**108\***) abstracts a hydrogen atom from an alkane or aldehyde substrate, resulting in the formation of a carbon-centered radical and a singly reduced decatungstate complex (**109**). The subsequent addition of the carbon-centered radical to alkenes generates alkyl extended radicals (**127**), which can reversibly react with Co(II) to form Co(III)-alkyl intermediates (**128**). Upon photo-irradiation, Co(III)-alkyl intermediates lead to alkene products and Co(III)-H through



Scheme 20 Decatungstate/Cu catalysed trifluoromethylation of sp<sup>3</sup> C-H bonds.



Scheme 22 Decatungstate/Co catalyzed site-selective alkenylation.

Scheme 23 Decatungstate/Cr catalyzed synthesis of  $\alpha$ -alkylated alcohols.

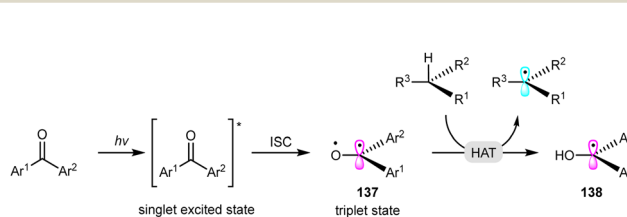
formal  $\beta$ -H elimination. The protonation of Co(III)-H facilitates the H<sub>2</sub> evolution, releasing a Co(III) complex. Final SET between the singly reduced decatungstate complex (**109**) and Co(III) complex ensures the regeneration of both catalysts ( $E_{1/2}[\text{W}_{10}\text{O}_{32}]^{4-}/[\text{W}_{10}\text{O}_{32}]^{5-} = -0.96 \text{ V vs. Ag/Ag}^+$  in MeCN,  $E_{1/2}(\text{Co}^{\text{III}}/\text{Co}^{\text{II}}) = -0.68 \text{ V vs. Ag/Ag}^+$  in MeCN). This methodology provides an efficient access to the alkenylated products of alkanes and aldehydes, displaying an exclusive *E* selectivity, and enables the late-stage alkenylation of natural products and their derivatives.

#### 4.5 Chromium catalysis

Yahata and co-workers reported the synthesis of  $\alpha$ -alkylated alcohols from aldehydes by merging decatungstate and chromium(III) trichloride (Scheme 23).<sup>110</sup> The SET reduction of chromium(III) trichloride by  $[\text{W}_{10}\text{O}_{32}]^{5-}\text{H}^+$  ( $\{E([\text{W}_{10}\text{O}_{32}]^{4-}/[\text{W}_{10}\text{O}_{32}]^{5-}) = -0.97 \text{ V vs. SCE}, E(\text{Cr}^{3+}/\text{Cr}^{2+}) = -0.65 \text{ V vs. SCE}\}$ ) generates chromium(II), which captures an alkyl radical to form an organochromium carbanion (**132**). The organochromium carbanion selectively reacts with aldehydes, yielding chromium alkoxides (**133**), followed by protonation to afford  $\alpha$ -alkylated alcohols. Inert alkanes, amides and ethers are all good substrates in this transformation.

## 5. Diaryl ketones (aryl aldehydes) as photocatalysts and HAT reagents

Diaryl ketones exhibit a prototypical reactivity in HAT processes, upon the generation of a long-lived triplet state (**137**) through the electron excitation from a non-bonding orbital at the C=O bond to a corresponding  $\pi^*$  orbital ( $n, \pi^*$ ) followed by intersystem crossing (ISC). Subsequent HAT with a  $sp^3$  C-H bond will generate an alkyl radical and ketyl radical (**138**) (Scheme 24).<sup>16</sup>

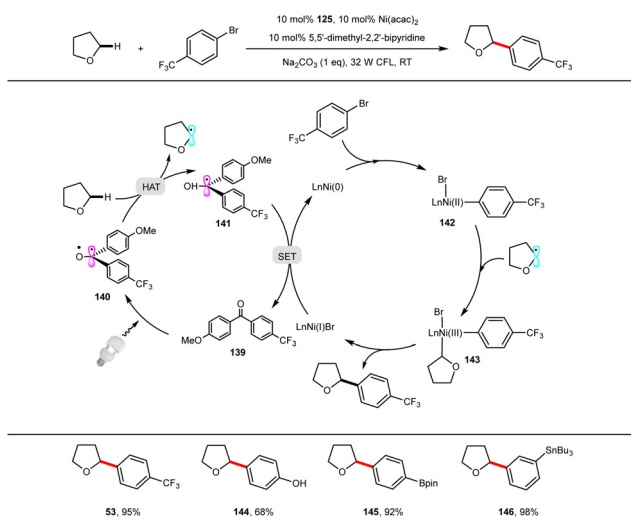


Scheme 24 The property of diaryl ketones under photo induction.

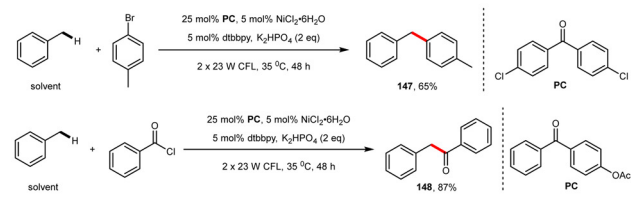
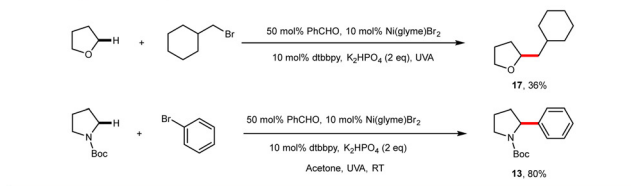
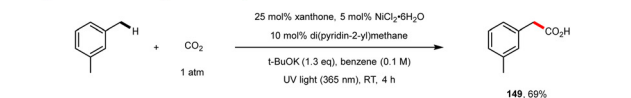
#### 5.1 Nickel catalysis

In 2018, Martin and co-workers successfully achieved the arylation, vinylation, and alkylation of ethers, amides, and benzylic alkanes using a combination of a diaryl ketone and nickel catalyst (Scheme 25a).<sup>111</sup> Remarkably, this reaction tolerates phenols, primary alcohols, amides, alkynes, alkenes, anilines, aldehydes, aryl boronates, and organostannanes as coupling partners. The coupling between an inert alkane, such as cyclohexane, and aryl bromides was also successful using this strategy. The authors discovered that diaryl ketones with a “push-pull” structure, characterized by an electron-donating substituent on one benzene backbone and an electron-withdrawing substituent on the other, provided higher yields compared to pure push or pull structure diaryl ketones. This improvement can be attributed to a higher molar absorption coefficient in the visible light region and the enhanced stability of the corresponding ketyl radical (**141**) with CF<sub>3</sub>-substituted analogs. Mechanistically, the redox potential of the ketyl radical (**141**) ( $E_{1/2}^{\text{red}} = -2.05 \text{ V vs. Ag/AgNO}_3$  in MeCN) allows for the generation of Ni(0) from Ni(II) ( $E_{\text{red}}(\text{Ni}^{\text{I}}/\text{Ni}^{\text{0}}) \approx -1.13 \text{ V vs. Ag/AgNO}_3$  in DMF).

In an independent study, Rueping and co-workers reported the arylation of benzylic C-H bonds using a diaryl ketone as a photosensitizer in combination with a nickel catalyst (Scheme 25b).<sup>112</sup> Iodoarenes, bromoarenes, and chloroarenes

a. Diaryl ketone mediated  $sp^3$  C-H functionalization

## b. Diaryl ketone mediated arylation and acylation of benzylic C-H

c. Benzaldehyde mediated  $sp^3$  C-H functionalizationd. Diaryl ketone mediated  $sp^3$  C-H carboxylation

Scheme 25 Diaryl ketone (aryl aldehyde)/Ni metallaphotoredox catalysis and applications.

are all suitable coupling partners. The observation of the bibenzyl and benzopinacol formation in the absence of a nickel catalyst and ligand supports the role of the diaryl ketone as a HAT catalyst in this reaction. The lower yields observed for iodoarenes compared to bromoarenes, along with the improved yields of iodoarenes after the addition of tetrabutyl ammonium bromide (TBAB), led the authors to propose an additional role for the diaryl ketone compound as an energy transfer agent. This energy transfer enables the homolysis of an aryl Ni(II) bromide species, generating a bromide radical. The bromide radical can then abstract a hydrogen atom from a hydrogen donor, thereby accelerating the transformation. The same research group subsequently reported the acylation of benzylic C-H bonds under similar conditions using acyl chlorides and anhydrides as coupling partners (Scheme 25b).<sup>113</sup> Hashmi and

co-workers employed a similar strategy, combining benzaldehyde and nickel, to achieve the  $\alpha$ -alkylation and arylation of ethers and amides, with benzaldehyde acting as a HAT catalyst (Scheme 25c).<sup>114,115</sup>

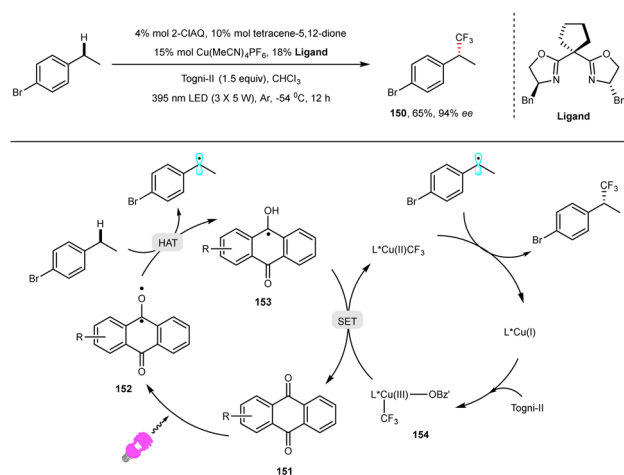
Furthermore, Murakami and co-workers reported the challenging carboxylation of C(sp<sup>3</sup>)-H bonds using xanthone as a photocatalyst and CO<sub>2</sub> as a carboxylate source in combination with a nickel catalyst (Scheme 25d).<sup>116</sup> This reaction was conducted under an atmospheric pressure of CO<sub>2</sub> at ambient temperature, enabling the direct conversion of readily available sp<sup>3</sup> C-H containing molecules, including benzylic alkanes, cyclohexane, and pentane, into their corresponding carboxylic acids with one carbon extension. These findings highlight the potential of the diaryl ketone/Ni strategy for the efficient carboxylation of sp<sup>3</sup> C-H bonds.

## 5.2 Copper catalysis

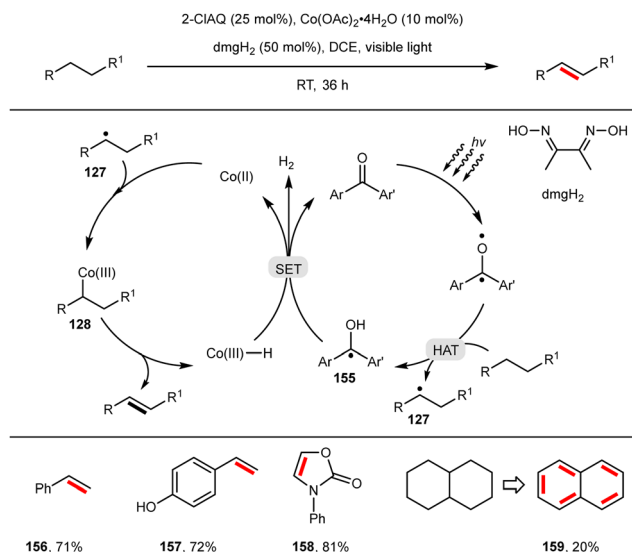
A notable development by Liu and co-workers involved the enantioselective trifluoromethylation of benzylic C-H bonds using 2-chloroanthracene-9,10-dione (2-ClAQ) and tetracene-5,12-dione as photocatalysts, in the conjunction with a copper catalyst and chiral ligand (Scheme 26).<sup>117</sup> The proposed mechanistic pathway begins with the oxidation of the L<sup>\*</sup>Cu(I) catalyst by Togni-II reagent, generating a L<sup>\*</sup>Cu(III)-CF<sub>3</sub> species (154). This species then undergoes a SET oxidation to the ketyl radical (153) formed *via* HAT, thus regenerating the photocatalyst. Simultaneously, the released L<sup>\*</sup>Cu(II)-CF<sub>3</sub> species selectively captures a benzylic radical, yielding the desired product in an enantioselective manner. This process likely involves the reductive elimination of an alkyl Cu(III)-CF<sub>3</sub> species. Control experiments support the presence of CF<sub>3</sub> radicals in the catalytic cycle, which are generated through the reversible homolytic cleavage of the L<sup>\*</sup>Cu(III)-CF<sub>3</sub> species (154).

## 5.3 Cobalt catalysis

Huang and co-workers have demonstrated an efficient method for the alkane dehydrogenation using a combination of readily



Scheme 26 Diaryl ketone/Cu catalysed benzylic C-H trifluoromethylation.

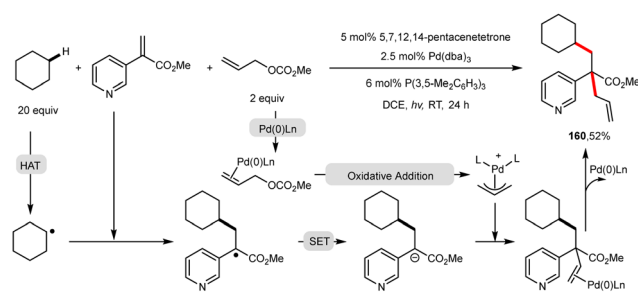


Scheme 27 Diaryl ketone/Co catalysed dehydrogenation of alkanes.

available and cost-effective cobalt salt Co(OAc)<sub>2</sub>·4H<sub>2</sub>O, low-cost dmgH<sub>2</sub>, and 2-CIAQ (Scheme 27).<sup>118</sup> Under photoexcitation, 2-CIAQ generates alkyl radicals, which are then captured by Co(II) to form Co(III)-alkyl intermediates (**128**). The subsequent β-hydrogen elimination of **128** leads to the formation of olefin products and Co(III)-H. The ketyl radical (**155**) undergoes SET with Co(III)-H, generating Co(II)-H and a protonated ketone. The protonated ketone is sufficiently acidic to protonate Co(II)-H, thereby regenerating Co(II) and 2-CIAQ while evolving H<sub>2</sub>. Notably, this transformation exhibits tolerances towards unprotected hydroxyl, amide, bromide, iodide, and borate functionalities. A broad range of alkane substrates, including (hetero)aryl-, thioether-, amide-, and carbonyl-substituents, can be dehydrogenated successfully. Multiple dehydrogenation events can also occur, as exemplified by the generation of naphthalene from decahydronaphthalene through penta-dehydrogenations. Furthermore, this strategy is applicable to the dehydrogenation of carbonyl compounds possessing benzylic or allylic β C-H bonds or β-heteroatom substituents.

#### 5.4 Palladium catalysis

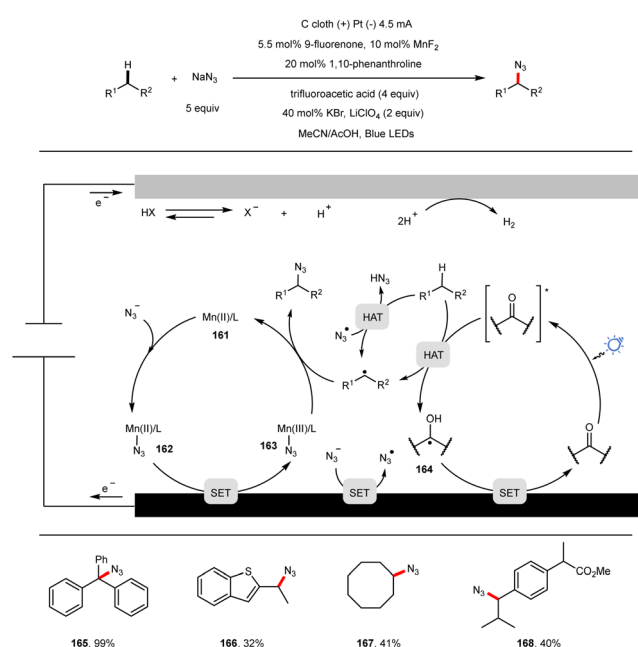
The allylic alkylation reaction, which involves the combination of π-allylpalladium electrophiles and carbon nucleophiles, is widely recognized as a highly effective method for the C-C bond formation.<sup>119,120</sup> Wang and co-workers have reported a three-component reaction utilizing C(sp<sup>3</sup>)-H substrates, electron-deficient terminal alkenes, and allyl carbonates. This transformation makes the use of 5,7,12,14-pentacenetetrone (PT) and a palladium phosphine catalyst (Scheme 28).<sup>121</sup> Importantly, this three-component coupling protocol exhibits a broad substrate compatibility, accommodating various terminal alkenes, aliphatic C-H bonds, and allyl carbonates. The application of this methodology has been demonstrated in the formal synthesis of mesembrine, showcasing its practical synthetic utility.



Scheme 28 Diaryl ketone/Pd catalysed three-component allylic alkylation.

#### 5.5 Manganese catalysis

In recent years, the integration of electrochemistry and photochemistry has emerged as a promising approach, expanding the repertoire of catalytic strategies for exploring challenging chemical transformations.<sup>122–124</sup> Given that the azide transfer from a Mn-N<sub>3</sub> complex to an alkyl radical can enable the formation of a C(sp<sup>3</sup>)-N<sub>3</sub> bond,<sup>125</sup> Lei and co-workers have developed an innovative electrophotocatalytic manganese-catalyzed oxidative azidation of C(sp<sup>3</sup>)-H bonds, accompanied by the clean release of H<sub>2</sub> as a side product (Scheme 29).<sup>126</sup> In this transformation, the anode facilitates the direct oxidation of sodium azide to generate the corresponding azide radical, while an azide anion and a ligand-coordinated Mn(II) complex (**162**) undergo an anodic oxidation, leading to the formation of a Mn(III)/L-N<sub>3</sub> intermediate (**163**). Alternatively, the Mn(III)/L-N<sub>3</sub> intermediate can also be accessed directly by the addition of the azido radical to the ligand-coordinated Mn(II) complex (**161**). The azide transfer from the Mn(III)/L-N<sub>3</sub> to alkyl radicals, generated through photoexcited diaryl ketone mediated HAT, results in the formation of alkyl azide products

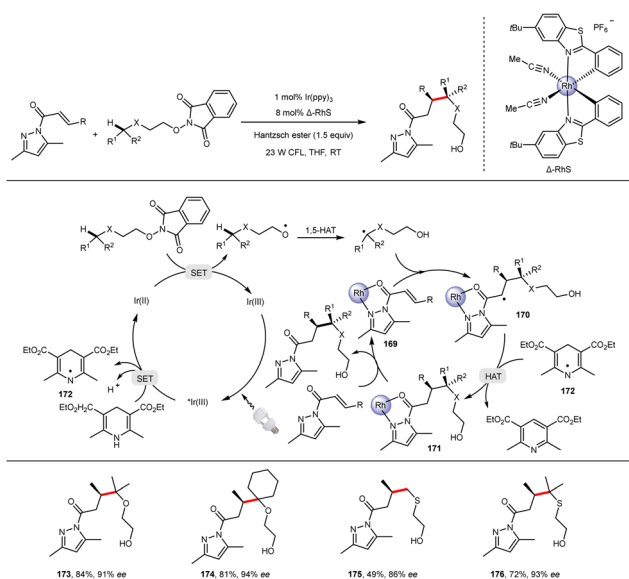
Scheme 29 Mn catalysed azidation of C(sp<sup>3</sup>)-H bonds under electro-photocatalysis.

and the release of the ligand-coordinated Mn(II) complex (**161**). The ketyl radical (**164**) can be regenerated by the anodic oxidation, restoring the initial photocatalyst. Notably, azide radicals may also perform HAT to alkanes. Additionally, the possibility of the Mn(III)/L-N<sub>3</sub> participating in the oxidation of the ketyl radical (**164**) to regenerate the photocatalyst can not be disregarded. This innovative protocol enables the introduction of an azide group to secondary and tertiary alkanes, demonstrating its potential for the late-stage azidation of valuable drug-like molecules.

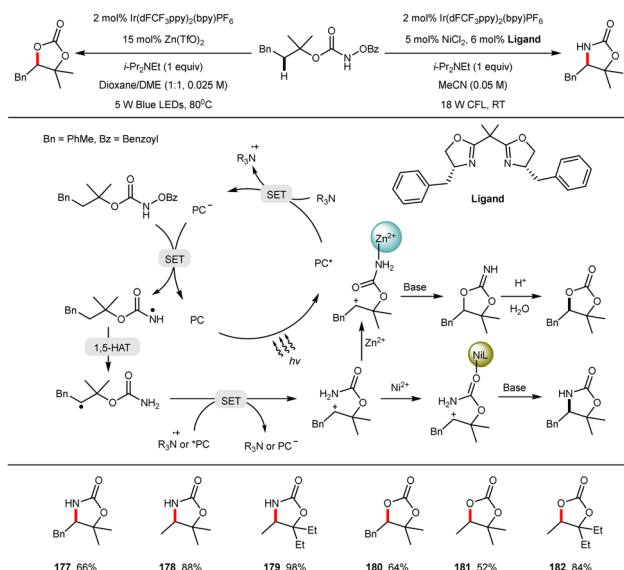
## 6. Transition metals as Lewis acid catalysts in HAT reactions

The use of chiral transition metal Lewis acid catalysts for asymmetric reactions has a long-standing and well-established history. Meggers and co-workers have reported an efficient asymmetric alkylation of  $\alpha,\beta$ -unsaturated *N*-acylpyrazoles using a chiral rhodium Lewis acid catalyst,  $\Delta$ -RhS (Scheme 30).<sup>127</sup> The addition of carbon-centered radicals to rhodium-coordinated *N*-acylpyrazoles (**169**) exhibit a remarkable enantioselectivity. The generated  $\alpha$ -carbonyl radicals (**170**) subsequently undergo hydrogen atom abstractions from dihydropyridine radicals (**172**), resulting in the formation of Rh-coordinated adducts (**171**). The ligand exchange with other *N*-acylpyrazole substrates leads to the release of highly enantioenriched products.

In this context, Lu and co-workers have demonstrated the controllable intramolecular C(sp<sup>3</sup>)-H amination and oxygenation of carbamates using NiCl<sub>2</sub> and Zn(OTf)<sub>2</sub> as Lewis acid catalysts, respectively (Scheme 31).<sup>128</sup> The chemoselectivity observed in this reaction can be rationalized by considering the different coordination preferences of carbamates with the metal ions. The Zn<sup>2+</sup> cation exhibits a preference for coordinating



**Scheme 30** Rhodium photoredox catalyzed asymmetric alkylation to double bonds.

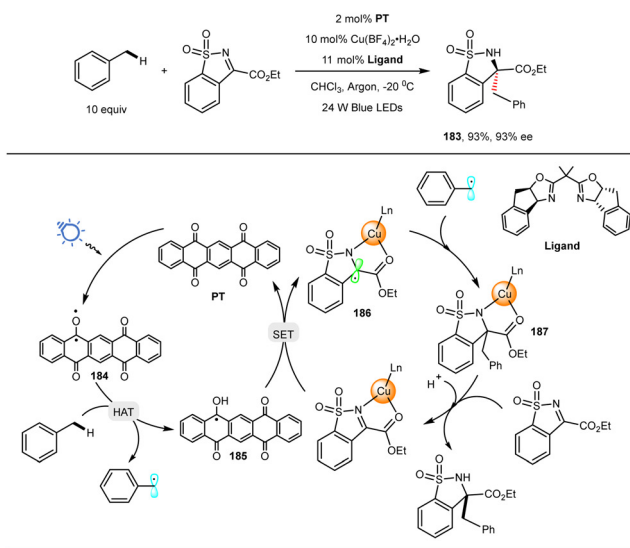


**Scheme 31** Nickel and zinc photoredox catalyzed amination and oxygenation of carbamates.

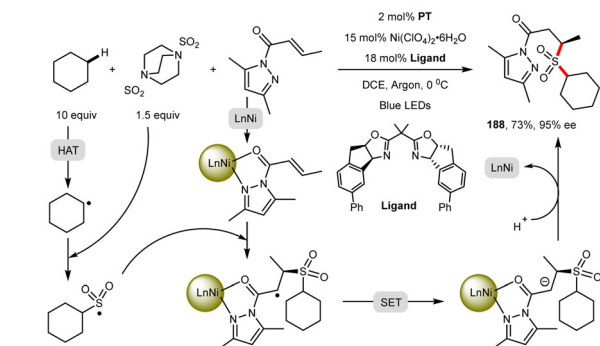
with the slightly “softer” nitrogen atom, whereas the Ni<sup>2+</sup> cation prefers the coordination with the slightly “harder” oxygen atom.

In another study, Gong and co-workers demonstrated the synergic cooperation of 5,7,12,14-pentacenetetrone (PT) and a chiral copper bisoxazoline complex for the coupling of sp<sup>3</sup> C-H bonds and *N*-sulfonylimines, leading to the formation of quaternary carbon stereocenters with a high enantioselectivity (Scheme 32a).<sup>129</sup> A diverse range of substrates including alkanes, cycloalkanes, toluene derivatives, and drug-like molecules were successfully converted into chiral *N*-sulfonylamine products. Mechanistically, photoexcited PT initiates HAT to the alkane substrate, generating an alkyl radical and a semi-quinone-type radical species (**185**). Subsequent SET between copper-coordinated *N*-sulfonylimine and **185** affords a tertiary radical complex (**186**) while regenerating PT. The cross-coupling between the alkyl radical and **186** yields a neutral complex (**187**) with the stereochemistry governed by the chiral bisoxazoline copper catalyst. Final protonation followed by the ligand exchange with another *N*-sulfonylimine results in the formation of the enantioenriched product. In a related work, the same group reported a three-component asymmetric sulfonation reaction involving C(sp<sup>3</sup>)-H precursors, a SO<sub>2</sub> surrogate, and  $\alpha,\beta$ -unsaturated carbonyl compounds, utilizing a chiral nickel bisoxazoline complex as the Lewis acid catalyst (Scheme 32b).<sup>130</sup>

Nagib and co-workers reported a noteworthy enantioselective sp<sup>3</sup> C-H amination of imidates using metallaphotoredox catalysis, leading to the synthesis of oxazolines (Scheme 33).<sup>131</sup> Oxime imidates can be obtained from aliphatic alcohols, and the generated oxazolines can be readily hydrolyzed to generate amino alcohols. Interestingly, due to the unfavorable redox potentials ( $E_{\text{red}} [0/-] = -1.6 \text{ V vs. SCE}$  for oxime imidates,  $E_{\text{red}} [\text{PC}/\text{PC}^-] = -1.4 \text{ V vs. SCE}$  for the photocatalyst) and the significant difference in triplet energies (62 kcal mol<sup>-1</sup> for the photocatalyst vs. 47 kcal mol<sup>-1</sup> for oxime

a. Chiral alkylation of *N*-sulfonylimines

## b. Three component asymmetric sulfonation reaction

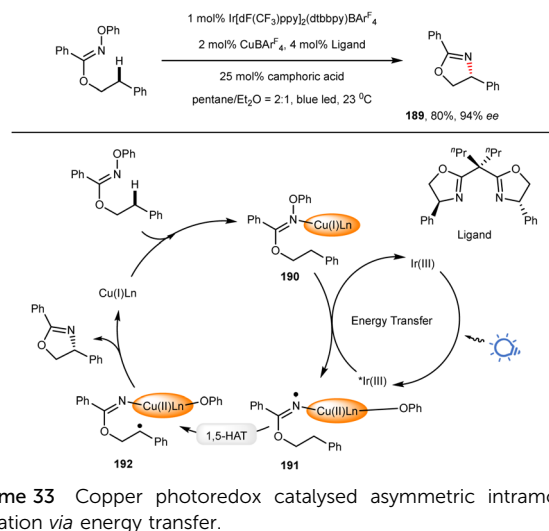


Scheme 32 Copper and nickel photoredox catalysed asymmetric addition to double bonds.

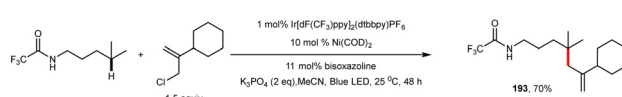
imidates), it is postulated that an energy transfer pathway is more plausible than an electron transfer process. In this context, chiral Cu(I) complex-coordinated imidates (**190**) undergo triplet energy transfer from the excited photocatalyst, leading to the formation of nitrogen-centered radicals (**191**). Subsequent 1,5-HAT affords carbon-centered radicals (**192**), which then undergo an intramolecular amination to yield enantioenriched oxazolines.

Alkenes possessing an allylic leaving group have conventionally been employed as allylation agents.<sup>132</sup> Tambar and co-workers introduced a novel approach for the remote allylation of C(sp<sup>3</sup>)-H bonds (Scheme 34a).<sup>133</sup> In this transformation, a proton-coupled electron transfer (PCET) process, followed by 1,5-HAT, generates a  $\delta$  carbon-centered radical from trifluoroacetamide. This radical subsequently adds to an allylic chloride substrate, leading to the formation of an alkyl allylation product. The inclusion of the Ni-catalyst in the reaction serves as a Lewis acid catalyst, effectively suppressing the undesired dimerization and photoisomerization of allylic chlorides.

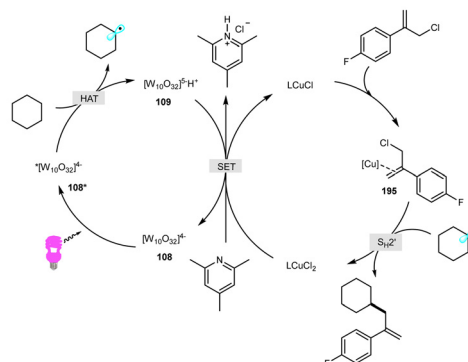
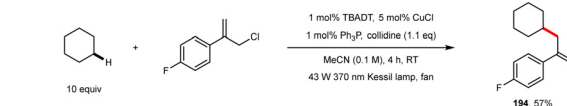
Another notable development in the field of the C(sp<sup>3</sup>)-H allylation of unactivated alkanes was achieved by Fañanás-Mastral and co-workers (Scheme 34b).<sup>134</sup> Their elegant protocol



Scheme 33 Copper photoredox catalysed asymmetric intramolecular amination via energy transfer.

a.  $\alpha$ -allylation of amides through 1,5-HAT

## b. Allylation of alkanes

Scheme 34 Nickel and copper photoredox catalysed allylation of sp<sup>3</sup> C-H bonds.

involves the utilization of TBADT as a HAT catalyst and CuCl as a transition metal catalyst. Notably, the HAT generated alkyl radical does not interact with the Cu(I) catalyst to form an alkyl-Cu(II) intermediate. Instead, it undergoes an addition to an allylic  $\pi$ -olefin-Cu(I) complex (**195**) through a S<sub>H</sub>2' pathway, affording the desired allylation product while concurrently generating a Cu(II) complex. The final step involves SET between the Cu(II) complex and singly reduced decatungstate ( $E_{1/2}(\text{CuCl}_2/\text{CuCl}) = +0.56 \text{ V vs. SCE}$ ;  $E_{1/2}[\text{W}_{10}\text{O}_{32}]^{4-}/[\text{W}_{10}\text{O}_{32}]^{5-} = -0.97 \text{ V vs. SCE}$ ), regenerating the Cu(I) catalyst and TBADT. This innovative protocol enables the efficient synthesis of a range of sp<sup>3</sup> C-H allylation structures, including those derived from natural products, with good yields.

## 7. Summary and outlook

In recent years, significant progress has been made in the field of  $sp^3$  C–H functionalizations through the combination of transition metal catalysis and various photocatalytic HAT processes. These methodologies have enabled the synthesis of complex drug molecules and natural products that were previously inaccessible using single photocatalysis or transition metal catalysis alone. Despite these achievements, the mechanisms of metallaphotoredox catalysis still need further clarifications. Often redox pathways are proposed but neither spectroscopic investigations nor DFT studies have been performed to support described reaction mechanisms. A better understanding of metallaphotoredox catalysis mechanisms will certainly be important for the advancement of the field and it will open up new applications relevant to green chemistry, drug synthesis, material science, and other related scientific fields. The concept of electrophotocatalysis, combining photocatalysis and electrocatalysis, has emerged as a powerful tool for organic synthesis.<sup>135–137</sup> This approach takes the advantage of the strengths of both methods, allowing accesses to novel reaction pathways that are otherwise inaccessible. Electrocatalytic redox reactions can replace chemical co-oxidants, enabling the recycling of reduced photocatalysts, while the electrocatalytic generation of photocatalysts from non-absorbing precursors facilitates high-energy redox reactions. By using electricity as the traceless redox agent, electrophotocatalysis may offer improved practicality, economy, safety, and sustainability. Although still an emerging and underexplored area, advances in electrocatalysis, photocatalysis, and the discovery of new electrochemically activated photocatalysts will undoubtedly provide new opportunities in the future. Biocatalysis, which harnesses the catalytic power of enzymes, offers a green and mild approach to organic synthesis. However, combining biocatalysis with electrocatalysis poses challenges such as the low regioselectivity, high overpotential, and electrode fouling. To overcome these limitations, the field of photobiocatalysis has emerged.<sup>138–140</sup> Photobiocatalysis utilizes the photoredox properties of oxidoreductases with metal clusters or organic moieties containing prosthetic groups, particularly metalloenzymes. Various photocatalysts have been developed to facilitate the electron transfer to the enzyme's prosthetic group or enable the indirect photocatalytic or electrocatalytic cofactor regeneration.<sup>141</sup> The discovery of new catalysts in photobiocatalysis holds promises for enabling the challenging transformations of C–H bonds into more reactive functional groups and developing chemo-enzymatic photoredox cascade reactions. In conclusion, the field of metallaphotoredox catalysis for the C–H activation and functionalization is a rapidly growing and highly promising area of research, with the significant potential for transformative developments in catalysis. The future will hold exciting possibilities for further advancements and breakthroughs in this field.

## Conflicts of interest

There are no conflicts to declare.

## Acknowledgements

J. Zhang thanks Jining Medical University High-Level Research Foundation (600497001, 600497002) for financial support.

## References

- 1 B. Li and Z. Shi, *Chem. Soc. Rev.*, 2012, **41**, 5588–5598.
- 2 Q. Zheng and N. Jiao, *Chem. Soc. Rev.*, 2016, **45**, 4590–4627.
- 3 J. A. Labinger, *Chem. Rev.*, 2017, **117**, 8483–8496.
- 4 Y. Yang, J. Lan and J. You, *Chem. Rev.*, 2017, **117**, 8787–8863.
- 5 C. G. Newton, S. Wang, C. C. Oliveira and N. Cramer, *Chem. Rev.*, 2017, **117**, 8908–8976.
- 6 Z. Dong, Z. Ren, S. J. Thompson, Y. Xu and G. Dong, *Chem. Rev.*, 2017, **117**, 9333–9403.
- 7 R. Shang, L. Ilies and E. Nakamura, *Chem. Rev.*, 2017, **117**, 9086–9139.
- 8 P. Gandeepan, T. Müller, D. Zell, G. Cera, S. Warratz and L. Ackermann, *Chem. Rev.*, 2019, **119**, 2192–2452.
- 9 R. R. Karimov and J. F. Hartwig, *Angew. Chem., Int. Ed.*, 2018, **57**, 4234–4241.
- 10 D. J. Abrams, P. A. Provencher and E. J. Sorensen, *Chem. Soc. Rev.*, 2018, **47**, 8925–8967.
- 11 O. Baudoin, *Angew. Chem., Int. Ed.*, 2020, **59**, 17798–17809.
- 12 J. He, M. Wasa, K. S. L. Chan, Q. Shao and J. Yu, *Chem. Rev.*, 2017, **117**, 8754–8786.
- 13 H. Yi, G. Zhang, H. Wang, Z. Huang, J. Wang, A. K. Singh and A. Lei, *Chem. Rev.*, 2017, **117**, 9016–9085.
- 14 Z. Chen, M. Rong, J. Nie, X. Zhu, B. Shi and J. Ma, *Chem. Soc. Rev.*, 2019, **48**, 4921–4942.
- 15 C. K. Prier, D. A. Rankic and D. W. C. MacMillan, *Chem. Rev.*, 2013, **113**, 5322–5363.
- 16 N. A. Romero and D. A. Nicewicz, *Chem. Rev.*, 2016, **116**, 10075–10166.
- 17 L. Capaldo and D. Ravelli, *Eur. J. Org. Chem.*, 2017, 2056–2071.
- 18 J. C. K. Chu and T. Rovis, *Angew. Chem., Int. Ed.*, 2018, **57**, 62–101.
- 19 L. M. Stateman, K. M. Nakafuku and D. A. Nagib, *Synthesis*, 2018, **50**, 1569–1586.
- 20 H. Cao, X. Tang, H. Tang, Y. Yuan and J. Wu, *Chem. Catal.*, 2021, **1**, 523–598.
- 21 J. Twilton, C. Le, P. Zhang, M. H. Shaw, R. W. Evans and D. W. C. MacMillan, *Nat. Rev. Chem.*, 2017, **1**, 0052.
- 22 C. Zhu, H. Yue, L. Chu and M. Rueping, *Chem. Sci.*, 2020, **11**, 4051–4064.
- 23 C. Zhu, H. Yue, J. Jia and M. Rueping, *Angew. Chem., Int. Ed.*, 2021, **60**, 17810–17831.
- 24 W. Yuan, S. Zheng and Y. Hu, *Synthesis*, 2020, **53**, 1719–1733.
- 25 F. Lu, G. He, L. Lu and W. Xiao, *Green Chem.*, 2021, **23**, 5379–5393.
- 26 T. Sarkar, T. A. Shah, P. K. Maharana, B. Debnath and T. Punniyamurthy, *Eur. J. Org. Chem.*, 2022, e202200541.

- 27 P. P. Singh, P. K. Singh and V. Srivastava, *Org. Chem. Front.*, 2023, **10**, 216–236.
- 28 Z. Ye, Y. Lin and L. Gong, *Eur. J. Org. Chem.*, 2021, 5545–5556.
- 29 P. L. Gkizis, *Eur. J. Org. Chem.*, 2022, e202201139.
- 30 H. Yue, C. Zhu, L. Huang, A. Dewanji and M. Rueping, *Chem. Commun.*, 2022, **58**, 171–184.
- 31 A. Y. Chan, I. B. Perry, N. B. Bissonnette, B. F. Buksh, G. A. Edwards, L. I. Frye, O. L. Garry, M. N. Lavagnino, B. X. Li, Y. Liang, E. Mao, A. Millet, J. V. Oakley, N. L. Reed, H. A. Sakai, C. P. Seath and D. W. C. MacMillan, *Chem. Rev.*, 2022, **122**, 1485–1542.
- 32 S. Z. Tasker, E. A. Standley and T. F. Jamison, *Nature*, 2014, **509**, 299–309.
- 33 L. Huang, T. Ji and M. Rueping, *J. Am. Chem. Soc.*, 2020, **142**, 3532–3539.
- 34 M. H. Shaw, V. W. Shurtleff, J. A. Terrett, J. D. Cuthbertson and D. W. C. MacMillan, *Science*, 2016, **352**, 1304–1308.
- 35 B. Maity, C. Zhu, H. Yue, L. Huang, M. Harb, Y. Minenkov, M. Rueping and L. Cavallo, *J. Am. Chem. Soc.*, 2020, **142**, 16942–16952.
- 36 C. Le, Y. Liang, R. W. Evans, X. Li and D. W. C. MacMillan, *Nature*, 2017, **547**, 79–83.
- 37 X. Zhang and D. W. C. MacMillan, *J. Am. Chem. Soc.*, 2017, **139**, 11353–11356.
- 38 J. Twilton, M. Christensen, D. A. DiRocco, R. T. Ruck, I. W. Davies and D. W. C. MacMillan, *Angew. Chem., Int. Ed.*, 2018, **57**, 5369–5373.
- 39 W. Guo, Q. Wang and J. Zhu, *Chem. Soc. Rev.*, 2021, **50**, 7359–7377.
- 40 S. M. Thullen, S. M. Treacy and T. Rovis, *J. Am. Chem. Soc.*, 2019, **141**, 14062–14067.
- 41 R. T. Simons, M. Nandakumar, K. Kwon, S. K. Ayer, N. M. Venneti and J. L. Roizen, *J. Am. Chem. Soc.*, 2023, **145**, 3882–3890.
- 42 Z. Ma, M. Li, L. Guo, L. Liu, D. Wang and X. Duan, *Org. Lett.*, 2021, **23**, 474–479.
- 43 Z. Zhang, L. M. Stateman and D. A. Nagib, *Chem. Sci.*, 2019, **10**, 1207–1211.
- 44 Z. Zhang, X. Zhang and D. A. Nagib, *Chem*, 2019, **5**, 3127–3134.
- 45 A. Hossain, A. Bhattacharyya and O. Reiser, *Science*, 2019, **364**, eaav9713.
- 46 X. Bao, Q. Wang and J. Zhu, *Angew. Chem., Int. Ed.*, 2019, **58**, 2139–2143.
- 47 X. Bao, Q. Wang and J. Zhu, *Chem. – Eur. J.*, 2019, **25**, 11630–11634.
- 48 H. Chen, W. Jin and S. Yu, *Org. Lett.*, 2020, **22**, 5910–5914.
- 49 L. M. Stateman, R. M. Dare, A. N. Paneque and D. A. Nagib, *Chem*, 2022, **8**, 210–224.
- 50 J. B. McManus, J. D. Griffin, A. R. White and D. A. Nicewicz, *J. Am. Chem. Soc.*, 2020, **142**, 10325–10330.
- 51 A. A. Isse, C. Y. Lin, M. L. Coote and A. Gennaro, *J. Phys. Chem. B*, 2011, **115**, 678–684.
- 52 G. N. Schrauzer, J. W. Sibert and R. J. Windgassen, *J. Am. Chem. Soc.*, 1968, **90**, 6681–6688.
- 53 M. E. Weiss, L. M. Kreis, A. Lauber and E. M. Carreira, *Angew. Chem., Int. Ed.*, 2011, **50**, 11125–11128.
- 54 X. Sun, J. Chen and T. Ritter, *Nat. Chem.*, 2018, **10**, 1229–1233.
- 55 H. Cao, H. Jiang, H. Feng, J. M. C. Kwan, X. Liu and J. Wu, *J. Am. Chem. Soc.*, 2018, **140**, 16360–16367.
- 56 J. H. Herbort, T. N. Bednar, A. D. Chen, T. V. RajanBabu and D. A. Nagib, *J. Am. Chem. Soc.*, 2022, **144**, 13366–13373.
- 57 L. Huang, T. Ji, C. Zhu, H. Yue, N. Zhumabay and M. Rueping, *Nat. Commun.*, 2022, **13**, 809.
- 58 Y. Okude, S. Hirano, T. Hiyama and H. Nozaki, *J. Am. Chem. Soc.*, 1977, **99**, 3179–3181.
- 59 H. Jin, J. Uenishi, W. J. Christ and Y. Kishi, *J. Am. Chem. Soc.*, 1986, **108**, 5644–5646.
- 60 K. Takai, M. Tagashira, T. Kuroda, K. Oshima, K. Utimoto and H. Nozaki, *J. Am. Chem. Soc.*, 1986, **108**, 6048–6050.
- 61 A. Fürstner and N. Shi, *J. Am. Chem. Soc.*, 1996, **118**, 12349–12357.
- 62 J. L. Schwarz, F. Schäfers, A. Tlahuext-Aca, L. Lückemeier and F. Glorius, *J. Am. Chem. Soc.*, 2018, **140**, 12705–12709.
- 63 H. Mitsunuma, S. Tanabe, H. Fuse, K. Ohkubo and M. Kanai, *Chem. Sci.*, 2019, **10**, 3459–3465.
- 64 S. Tanabe, H. Mitsunuma and M. Kanai, *J. Am. Chem. Soc.*, 2020, **142**, 12374–12381.
- 65 X. Peng, Y. Hirao, S. Yabu, H. Sato, M. Higashi, T. Akai, S. Masaoka, H. Mitsunuma and M. Kanai, *J. Org. Chem.*, 2023, **88**, 6333–6346.
- 66 P. Zhang, C. Le and D. W. C. MacMillan, *J. Am. Chem. Soc.*, 2016, **138**, 8084–8087.
- 67 D. R. Heitz, J. C. Tellis and G. A. Molander, *J. Am. Chem. Soc.*, 2016, **138**, 12715–12718.
- 68 S. K. Kariofillis, S. Jiang, A. M. Żurański, S. S. Gandhi, J. I. Martinez Alvarado and A. G. Doyle, *J. Am. Chem. Soc.*, 2022, **144**, 1045–1055.
- 69 D. Sun and A. G. Doyle, *J. Am. Chem. Soc.*, 2022, **144**, 20067–20077.
- 70 A. Rand, H. Yin, L. Xu, J. Giacoboni, R. Martin-Montero, C. Romano, J. A. Montgomery and R. Martin, *ACS Catal.*, 2020, **10**, 4671–4676.
- 71 A. Rand, M. Chen and J. A. Montgomery, *Chem. Sci.*, 2022, **13**, 10566–10573.
- 72 L. Huang, M. Szewczyk, R. Kancherla, B. Maity, C. Zhu, L. Cavallo and M. Rueping, *Nat. Commun.*, 2023, **14**, 548.
- 73 C. Huang, J. Li and C. Li, *Nat. Commun.*, 2021, **12**, 4010.
- 74 M. Jouffroy, C. B. Kelly and G. A. Molander, *Org. Lett.*, 2016, **18**, 876–879.
- 75 B. A. Vara, X. Li, S. Berritt, C. R. Walters, E. J. Petersson and G. A. Molander, *Chem. Sci.*, 2018, **9**, 336–344.
- 76 H. Li, L. Guo, X. Feng, L. Huo, S. Zhu and L. Chu, *Chem. Sci.*, 2020, **11**, 4904–4910.
- 77 L. Troian-Gautier, M. D. Turlington, S. A. M. Wehlin, A. B. Maurer, M. D. Brady, W. B. Swords and G. J. Meyer, *Chem. Rev.*, 2019, **119**, 4628–4683.
- 78 K. P. S. Cheung, S. Sarkar and V. Gevorgyan, *Chem. Rev.*, 2022, **122**, 1543–1625.

- 79 L. Chang, Q. An, L. Duan, K. Feng and Z. Zuo, *Chem. Rev.*, 2022, **122**, 2429–2486.
- 80 S. J. Hwang, D. C. Powers, A. G. Maher, B. L. Anderson, R. G. Hadt, S. Zheng, Y. Chen and D. G. Nocera, *J. Am. Chem. Soc.*, 2015, **137**, 6472–6475.
- 81 S. J. Hwang, B. L. Anderson, D. C. Powers, A. G. Maher, R. G. Hadt and D. G. Nocera, *Organometallics*, 2015, **34**, 4766–4774.
- 82 B. J. Shields and A. G. Doyle, *J. Am. Chem. Soc.*, 2016, **138**, 12719–12722.
- 83 S. K. Kariofillis and A. G. Doyle, *Acc. Chem. Res.*, 2021, **54**, 988–1000.
- 84 M. K. Nielsen, B. J. Shields, J. Liu, M. J. Williams, M. J. Zacuto and A. G. Doyle, *Angew. Chem., Int. Ed.*, 2017, **56**, 7191–7194.
- 85 L. K. G. Ackerman, J. I. Martinez Alvarado and A. G. Doyle, *J. Am. Chem. Soc.*, 2018, **140**, 14059–14063.
- 86 X. Cheng, H. Lu and Z. Lu, *Nat. Commun.*, 2019, **10**, 3549.
- 87 S. K. Kariofillis, B. J. Shields, M. A. Tekle-Smith, M. J. Zacuto and A. G. Doyle, *J. Am. Chem. Soc.*, 2020, **142**, 7683–7689.
- 88 M. S. Santos, A. G. Corrêa, M. W. Paixão and B. König, *Adv. Synth. Catal.*, 2020, **362**, 2367–2372.
- 89 X. Cheng, T. Li, Y. Liu and Z. Lu, *ACS Catal.*, 2021, **11**, 11059–11065.
- 90 Q. Wang, Z. Sun, H. Huang, G. Mao and G. Deng, *Green Chem.*, 2022, **24**, 3293–3299.
- 91 H. Deng, X. Fan, Z. Chen, Q. Xu and J. Wu, *J. Am. Chem. Soc.*, 2017, **139**, 13579–13584.
- 92 G. S. Lee, J. Won, S. Choi, M. Baik and S. H. Hong, *Angew. Chem., Int. Ed.*, 2020, **59**, 16933–16942.
- 93 L. Huang and M. Rueping, *Angew. Chem., Int. Ed.*, 2018, **57**, 10333–10337.
- 94 R. Kancherla, K. Muralirajan, B. Maity, S. Karuthedath, G. S. Kumar, F. Laquai, L. Cavallo and M. Rueping, *Nat. Commun.*, 2022, **13**, 2737.
- 95 J. Zhang, Y. Niu, F. Kong and M. Yan, *J. Catal.*, 2022, **416**, 58–67.
- 96 V. D. Waele, O. Poizat, M. Fagnoni, A. Bagno and D. Ravelli, *ACS Catal.*, 2016, **6**, 7174–7182.
- 97 L. Capaldo, D. Ravelli and M. Fagnoni, *Chem. Rev.*, 2022, **122**, 1875–1924.
- 98 I. B. Perry, T. F. Brewer, P. J. Sarver, D. M. Schultz, D. A. DiRocco and D. W. C. MacMillan, *Nature*, 2018, **560**, 70–75.
- 99 B. Maity, C. Zhu, M. Rueping and L. Cavallo, *ACS Catal.*, 2021, **11**, 13973–13982.
- 100 S. Xu, H. Chen, Z. Zhou and W. Kong, *Angew. Chem., Int. Ed.*, 2021, **60**, 7405–7411.
- 101 D. Mazzarella, A. Pulcinella, L. Bovy, R. Broersma and T. Noël, *Angew. Chem., Int. Ed.*, 2021, **60**, 21277–21282.
- 102 V. Murugesan, A. Ganguly, A. Karthika and R. Rasappan, *Org. Lett.*, 2021, **23**, 5389–5393.
- 103 T. Furuya, A. S. Kamlet and T. Ritter, *Nature*, 2011, **473**, 470–477.
- 104 A. J. Hickman and M. S. Sanford, *Nature*, 2012, **484**, 177–185.
- 105 P. J. Sarver, V. Bacauanu, D. M. Schultz, D. A. DiRocco, Y. Lam, E. C. Sherer and D. W. C. MacMillan, *Nat. Chem.*, 2020, **12**, 459–467.
- 106 J. Ruan, O. Saidi, J. A. Iggo and J. Xiao, *J. Am. Chem. Soc.*, 2008, **130**, 10510–10511.
- 107 L. Wang, T. Wang, G. Cheng, X. Li, J. Wei, B. Guo, C. Zheng, G. Chen, C. Ran and C. Zheng, *ACS Catal.*, 2020, **10**, 7543–7551.
- 108 J. G. West, D. Huang and E. J. Sorensen, *Nat. Commun.*, 2015, **6**, 10093.
- 109 H. Cao, Y. Kuang, X. Shi, K. L. Wong, B. B. Tan, J. M. C. Kwan, X. Liu and J. Wu, *Nat. Commun.*, 2020, **11**, 1956.
- 110 K. Yahata, S. Sakurai, S. Hori, S. Yoshioka, Y. Kaneko, K. Hasegawa and S. Akai, *Org. Lett.*, 2020, **22**, 1199–1203.
- 111 Y. Shen, Y. Gu and R. Martin, *J. Am. Chem. Soc.*, 2018, **140**, 12200–12209.
- 112 A. Dewanji, P. E. Krach and M. Rueping, *Angew. Chem., Int. Ed.*, 2019, **58**, 3566–3570.
- 113 P. E. Krach, A. Dewanji, T. Yuan and M. Rueping, *Chem. Commun.*, 2020, **56**, 6082–6085.
- 114 L. Zhang, X. Si, Y. Yang, M. Zimmer, S. Witzel, K. Sekine, M. Rudolph and A. S. K. Hashmi, *Angew. Chem., Int. Ed.*, 2019, **58**, 1823–1827.
- 115 X. Si, L. Zhang and A. S. K. Hashmi, *Org. Lett.*, 2019, **21**, 6329–6332.
- 116 N. Ishida, Y. Masuda, Y. Imamura, K. Yamazaki and M. Murakami, *J. Am. Chem. Soc.*, 2019, **141**, 19611–19615.
- 117 P. Xu, W. Fan, P. Chen and G. Liu, *J. Am. Chem. Soc.*, 2022, **144**, 13468–13474.
- 118 M. Zhou, L. Zhang, G. Liu, C. Xu and Z. Huang, *J. Am. Chem. Soc.*, 2021, **143**, 16470–16485.
- 119 B. M. Trost and M. L. Crawley, *Chem. Rev.*, 2003, **103**, 2921–2944.
- 120 S. Norsikian and C. Chang, *Curr. Org. Synth.*, 2009, **6**, 264–289.
- 121 Y. Shen, Z. Dai, C. Zhang and P. Wang, *ACS Catal.*, 2021, **11**, 6757–6762.
- 122 J. P. Barham and B. König, *Angew. Chem., Int. Ed.*, 2020, **59**, 11732–11747.
- 123 Y. Yu, P. Guo, J. Zhong, Y. Yuan and K. Ye, *Org. Chem. Front.*, 2020, **7**, 131–135.
- 124 J. Liu, L. Lu, D. Wood and S. Lin, *ACS Cent. Sci.*, 2020, **6**, 1317–1340.
- 125 X. Huang, T. M. Bergsten and J. T. Groves, *J. Am. Chem. Soc.*, 2015, **137**, 5300–5303.
- 126 L. Niu, C. Jiang, Y. Liang, D. Liu, F. Bu, R. Shi, H. Chen, A. D. Chowdhury and A. Lei, *J. Am. Chem. Soc.*, 2020, **142**, 17693–17702.
- 127 C. Wang, K. Harms and E. Meggers, *Angew. Chem., Int. Ed.*, 2016, **55**, 13495–13498.
- 128 Q. Guo, X. Ren and Z. Lu, *Org. Lett.*, 2019, **21**, 880–884.
- 129 Y. Li, M. Lei and L. Gong, *Nat. Catal.*, 2019, **2**, 1016–1026.
- 130 S. Cao, W. Hong, Z. Ye and L. Gong, *Nat. Commun.*, 2021, **12**, 2377.
- 131 K. M. Nakafuku, Z. Zhang, E. A. Wappes, L. M. Stateman, A. D. Chen and D. A. Nagib, *Nat. Chem.*, 2020, **12**, 697–704.
- 132 K. Wu, L. Wang, S. Colón-Rodríguez, G. Flechsig and T. Wang, *Angew. Chem., Int. Ed.*, 2019, **58**, 1774–1778.

- 133 B. Xu and U. K. Tambar, *ACS Catal.*, 2019, **9**, 4627–4631.
- 134 P. Martínez-Balart, B. I. Tóth, Á. Velasco-Rubio and M. Fañanás-Mastral, *Org. Lett.*, 2022, **24**, 6874–6879.
- 135 P. Li, T. Zhang, M. Mushtaq, S. Wu, X. Xiang and D. Yan, *Chem. Rec.*, 2021, **21**, 841–857.
- 136 T. Hardwick and N. Ahmed, *ACS Sustainable Chem. Eng.*, 2021, **9**, 4324–4340.
- 137 H. Huang, K. A. Steiniger and T. H. Lambert, *J. Am. Chem. Soc.*, 2022, **144**, 12567–12583.
- 138 S. Lee, D. Choi, S. Kuk and C. Park, *Angew. Chem., Int. Ed.*, 2018, **57**, 7958–7985.
- 139 L. Schmermund, V. Jurkaš, F. F. Özgen, G. D. Barone, H. C. Büchenschütz, C. Winkler, S. Schmidt, R. Kourist and W. Kroutil, *ACS Catal.*, 2019, **9**, 4115–4144.
- 140 Y. Peng, Z. Chen, J. Xu and Q. Wu, *Org. Process Res. Dev.*, 2022, **26**, 1900–1913.
- 141 J. A. Bau, A. H. Emwas, P. Nikolaienko, A. A. Aljarb, V. Tung and M. Rueping, *Nat. Catal.*, 2022, **5**, 397–404.